

# Measuring the Frequency Response Function of X-braced Guitar Top and Guitar

A Thesis

Submitted by

Dan Luo

In partial fulfillment of the requirements for the degree of  
Master of Science  
In  
Mechanical Engineering

Department of Mechanical Engineering  
Tufts University  
May 2016

Committee members:

Chris Rogers

Robert White

Paul Lehrman

## Abstract

In this study, we measured the frequency response of an X-braced guitar top board and a fully constructed guitar. The top was fixed on an aluminum rig and excited by an impact hammer. A microphone recorded the radiated sound. Our Labview VIs analyzed the spectrums of both the input and output signal. Then we evaluated the frequency response from these two spectrums. The fundamental resonance of the fully braced guitar top board is about 173 Hz. We also measured the effect of this bracing pattern, which could potentially suppress lower modes and even the response at higher frequencies. The result from measuring the guitar top does not show strong agreement with theoretical calculations. A major reason might be the non-uniform boundary condition applied.

We also tested a fully-constructed guitar with the same top bracing configuration to investigate the effects of the guitar body. The influence of the soundhole, back, and string tension was also measured. The most significant effect of the body was that it significantly boosted the response at lower frequencies and an additional breathing mode also appeared in the spectrum. Data for measuring the fully constructed guitar has good agreement with past studies, where the two distinct responses were captured around 100 Hz (soundhole mode) and 200 Hz (plate mode). We tested the effect of the soundhole by covering it with the cardboard, which dramatically reduced the response of the breathing mode, and the plate response also shifted to lower frequencies. We added clay tablets on the back plate to investigate its effect on the guitar frequency response. This led the breathing mode to shift to lower frequencies. This shift had its maximum value when the additional weight concentrated on the center of the back plate. The guitar was also tested without string tensions, which results in a slight change in fundamental plate mode.

## Acknowledgement

I would firstly like to thank my thesis advisor Dr. Chris Rogers from the Department of Mechanical Engineering. He's always available to me to solving my problems, and many times he helped me to keep my research in the right direction.

I would also like to thank my committee members: Dr. Robert White and Dr. Paul Lehrman. Their expert knowledge provided many invaluable suggestions and comments.

I was enjoying in Dr. Mark Moller and Dr. Jim Moore's Acoustic class, which helped me established a strong technical foundation in my research.

I was in Mr Walter Stanul's musical instrument making class at the School of Museum and Fine Arts. His experiences greatly helped me to narrow down my research topic.

I was talking with Fan Tao from d'Addario on the phone. His experiences in the musical instrument industry provided me many useful perspectives.

I would also like to thank Collings Guitars from Austin, TX, who generously provided the guitar top board for my study.

<b>Abstract.....</b>	<b>i</b>
<b>Acknowledgement.....</b>	<b>ii</b>
<b>Table of Content.....</b>	<b>iii</b>
<b>List of Tables.....</b>	<b>iv</b>
<b>List of Figures.....</b>	<b>iv</b>
<b>Chapter 1 Introduction.....</b>	<b>1</b>
<b>Chapter 2 Literature Review</b>	
<b>2.1 Fundamental Concepts in Acoustics and Vibrations .....</b>	<b>14</b>
<b>2.2 Modeling Guitar as Coupled Mechanical System.....</b>	<b>24</b>
<b>Chapter 3 Methodology and Preparation</b>	
<b>3.1 Signal Processing Methodology.....</b>	<b>32</b>
<b>3.2 Experiment Preparation.....</b>	<b>38</b>
<b>Chapter 4 Result and Discussion</b>	
<b>4.1 Result.....</b>	<b>44</b>
<b>4.2 Discussion.....</b>	<b>61</b>
<b>Conclusion .....</b>	<b>68</b>
<b>Future Work .....</b>	<b>69</b>

## List of Tables

Table 1.1 Stiffness to density ratio of materials used to make acoustic guitar tops.....	1
Table 2.2.1 Important values for an air-body couple guitar model.....	28
Table 3.2.1 List of test equipment.....	40
Table 4.1.1 Testing Parameters .....	45
Table 4.2.1 Estimation of the fundamental mode using circular & fixed boundary assumption.....	60
Table 4.2.2 Q factor of the sound hole mode at various distance.....	62
Table 4.2.3 Q factor of the Plate mode at various distance.....	63
Table 4.2.4 Comparison of the presence of the soundhole.....	64
Table 4.2.5 Q factor when the microphone was placed in the soundhole.....	64

## List of Figures

Figure 1.1 Block-diagram represents a guitar as a mechanical system.....	2
Figure 1.2 First natural frequency from guitars with different back and side materials...5	
Figure 1.3 Comparison of the initial decay between a high quality and low quality guitar.....	7
Figure 1.4 Bracing on the back of the top .....	8
Figure 1.5 Shape of a scalloped bracing.....	9
Figure 1.6.Near-field measurement for the guitar FRF.....	10
Figure 1.7 Mode shapes from applying oscillating forces with different frequencies...12	
Figure 1.8 Comparison between contact method and ultrasound excitation method.....	13
Figure 2.1.1 Mode shape with nodal circles and nodal diameters.....	17
Figure 2.1.2 Vibration of plate from numerical simulation.....	17

Figure 2.2.1 Guitar as a reflex enclosure .....	24
Figure 2.2.2 First two mode of an acoustic guitar.....	27
Figure 2.2.3 Two degree freedom system of a guitar model .....	28
Figure 2.2.4 Effect of the back plate motion to guitar FRF .....	29
Figure 2.2.5 Equivalent circuit for an acoustic guitar .....	30
Figure 3.1.1 Block diagram of a measurement configuration.....	31
Figure 3.1.2 Output signal to an impulse input.....	33
Figure 3.1.3 Impulse response function having more than one frequency.....	34
Figure 3.1.4 Frequency domain representation of damped multi-modes signal.....	35
Figure 3.2.1 Guitar board tested in this study.....	39
Figure 3.2.2 Quiet chamber built for the frequency response measurement.....	39
Figure 3.2.3 Experiment setup.....	41
Figure 4.1.1 Top plate response and room noise response .....	44
Figure 4.1.2 Hammer frequency response .....	45
Figure 4.1.3 Frequency response of guitar board at different times.....	47
Figure 4.1.4 Excitation location .....	47
Figure 4.1.5 Guitar top response picked up at different locations.....	48
Figure 4.1.6 FRF from different brace configurations (50 Hz -1000 Hz).....	50
Figure 4.1.7 FRF from different brace configurations (1000Hz -3000Hz).....	50
Figure 4.1.8 FRF from a fully construct guitar.....	51
Figure 4.1.9 FRF measured at 5cm.....	52
Figure 4.1.10 FRF measured at 30 cm .....	53
Figure 4.1.11 FRF measured at 50 cm .....	54

Figure 4.1.12 Effect of covering the soundhole.....	55
Figure 4.1.13 Effect of placing microphone inside the guitar.....	55
Figure 4.1.14 Back plate treatments.....	56
Figure 4.1.15 FRF when the back is damped by clay bars.....	56
Figure 4.1.16 FRF with without muting the strings .....	57
Figure 4.1.17 Effect of the string tension.....	58
Figure 4.2.1 Assumed vibrational area of the guitar top .....	59
Figure 4.2.2 FRF of the top and guitar.....	61
Figure 4.2.3 Time-domain signal of the board and guitar signal.....	62
Figure 4.2.4 Error in guitar board measurement.....	66
Figure 4.2.5 Error in guitar measurement.....	66

## **Chapter 1 Introduction**

Based on the 2014 annual report from the National Association of Music Merchants (NAMM), fretted instrument (which includes acoustic guitar, electric guitar, and ukulele) has the highest industry revenue in the US. Among them, acoustic guitar has the highest sales, where total 1.3 million units were shipped in 2013. This data indicated acoustic guitar is one of most popular musical instruments in the US.

The modern steel string guitar has become a symbol of the popular music since the early 20th century. Musicians such as Robert Johnson, Elvis Presley, Bob Dylan and The Beatles all have their classics written and played with acoustic guitars. On a guitar the musical notes are generated by plucking the strings and the pitch will be determined by the string length, material density, string diameter, and the tension applied to the string. Different pitches are achieved by pressing the string at different fret locations so that the string length is changed. The vibration of a string could be modeled by the one-dimensional wave equation [12] [18], which could mathematically determine the pitch on a given string configuration.

Similar to other string instruments, the mechanism for a guitar to generate sound is the transmission of the string vibration energy to the guitar body, which finally radiates the acoustic sound to the surrounding areas [12] [18]. There are objective and subjective measures to evaluate the sound quality of a guitar. However, it is hard to apply a universal criterion to classify good and bad guitars. However, these subjective judgments are all representations of the physical properties of the instrument. For instance, if we say a guitar is much louder than another one, we may refer its efficiency on transmitting the string vibration to the sound waves. If we say a guitar has a warmer sound, we may speak



about its harmonic contents, which may have more energy in the low-mid frequency ranges.

The motivation of this study was trying to provide those subjective interpretations quantitative evidence so that both players and guitar makers could have deeper understandings on the instrument and potentially improve their skills in playing and making the instrument. Because the guitar has a relatively complicated structure, it is hard to evaluate its dynamics in an analytical method. Also, because the materials are not homogeneous over the entire area, thus we choose to analyze its dynamical behaviors through direct measurement.

This research is trying to test a methodology for obtaining the frequency response function of an X-braced (cross braced) guitar board and a fully constructed guitar with same bracing configuration. A microphone will directly record the acoustic data. The analysis is then accomplished by using our Labview VIs to show the acoustic characteristics of the testing instrument. The objective of this study is to come up with a simple and accurate method to measure the guitar frequency response. The physical interpretation based on the frequency response will also be provided. If this method could successfully characterize the dynamical behavior of the guitar board and the fully constructed guitar, then guitar makers can test their design before complete the instrument, the guitar player is also able to modify their instruments as they wish.

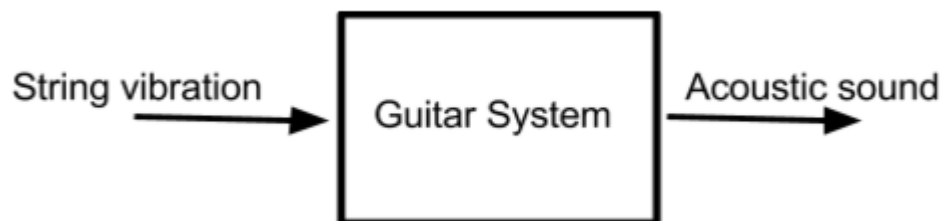


**Figure 1.1** Block diagram represents a guitar as a mechanical system

A guitar could be treated as a mechanical system, where the input is the string vibration and the output is the radiated sound (Figure 1.1). The string vibration feeds the mechanical energy to the guitar body through the bridge, then the body of the guitar excites the surrounding air to vibrate so that we can hear the sound [12] [19]. So between the string vibration and the radiated acoustic sound is called the response of the guitar, which both have time-domain property and frequency domain property. The response in time-domain can show how fast the system can respond to the input signal and decay. The frequency-domain information property will show the distribution of the output energy based on their frequencies.

We assume this mechanical system is Linear-Time-Invariant system [9] [18], which simply means the response of the guitar will not change with time, and the total output could be decomposed into a linear combination of different outputs with corresponding inputs. The output of the system will be simply a function of the input and the response of the guitar so that we can write the output function as:

$$f_{out} = f(F_{in}, h(t))$$

where  $h(t)$  is the guitar impulse response. In this case, we treated the guitar as a black box, which hides all the details inside the guitar system and its behavior could be evaluated by comparing the output signal and the input signal.

Guitar makers and musicians think the instrument will sound different after a longer period, which is mainly from the permanent property changes. For example, the string tension will induce permanent deformation of the body, which also could modify its stiffness. However, in this study, we assume this time is not long enough (less than a

month) to cause significant permanent deformations. Therefore, we could eliminate this effect in the analysis.

Among these system functions, the only unknown is the guitar response function  $h(t)$ , which is primarily determined by the mechanical properties of the material and the structure. However, it is difficult to evaluate the guitar response from its physical properties accurately. Therefore experimental methods need to be introduced to measure the response of the guitar.

The acoustic quality or the tone of the guitar could be determined by its frequency response function based on the magnitude and the shape of these resonance peaks. To obtain the frequency response, we need to transform the time domain signal to the frequency domain, and the well-known Fourier transform will perform this task. After we obtained the frequency response from both the input and output signal, then we can evaluate the system response of the guitar, which is the ratio between output frequency response and the input frequency response.

In this study, we were trying to obtain some quantitative measurements that could represent the property of a guitar. However, before we dive into those numbers, it is worth to describe some of the qualitative judgment regarding the quality of the guitar. Even though nowadays the manufacturing process of the guitar has been standardized by many companies, which eliminated significant quality variations, large variations were still observed from using different materials. Figure 1.2 shows the variation in the first resonance frequency of guitars with different materials. Theoretically, the resonance frequency is primarily controlled by the mechanical properties of the material, especially the stiffness and the density. For example, in Figure 1.2 rosewood displays a relatively

consistent resonance frequency. However, ovangkol shows a very wide range of the frequency responses. Also, the complicated structure and non-homogenous property distributions can all add difficulties to analyze the guitar response.

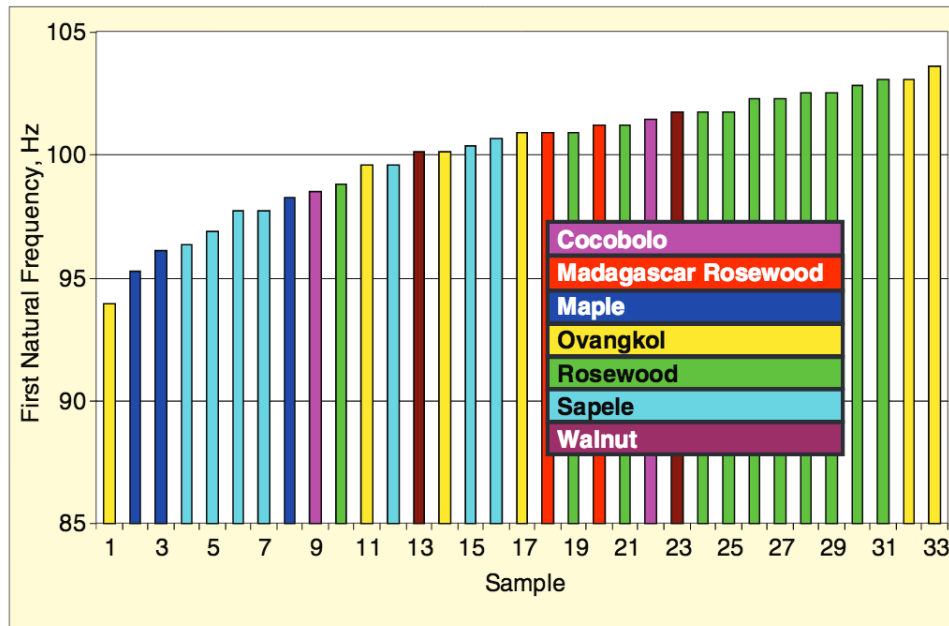


Figure 1.2 First natural frequencies from guitars with different back and side materials (Source: French [5])

Because of the nature of the wood, it is impossible to find two identical instruments. Moreover, there is also not a universal standard to evaluate the quality of musical instruments. However, through history, both guitar makers and players have found some common ground to say about the quality of the guitars. Terms like “balanced”, “warm”, “good articulations” or “good sustain” commonly see in guitar commercials. For example, Martin claimed their D-28 model has “Massive bass response balanced with articulate highs.”

In fact, all these subjective terms are referring the frequency response of the instrument. “Balanced” means the guitar has an even response at low, mid and high-frequency ranges and “massive bass response” indicates the guitar will have more energy in the low-

frequency ranges. Articulation usually appears as distinct peaks in specific frequency ranges; this is especially important at higher frequencies due to the higher modal density and high energy losses.

Some researchers tried to give some criteria on how to evaluate the quality of a guitar, criteria such as higher amplitude and lower frequency of the first mode [2] [4] (the breathing mode). The high amplitude usually is controlled by the mass, stiffness, and area of the top. A common understanding of this is that the amplitude is inversely related to the mass of the top and proportional to the effective area of the top (Christensen [4]). Therefore, the practical approach would be to select guitar top material with high stiffness to density ratio because an increase of the surface area will reduce the strength of the guitar top.

Another parameter was considered in evaluating the quality of the guitar is the initial decay of the sound, Caldersmith [2] concluded that higher quality guitar tends to have higher response and faster initial decay than low-quality guitars (Figure 1.3). The initial amplitude is greater for the high-quality guitar, but the decay time is same for both guitars, and this indicates a faster decay rate of the high-quality guitar.

Many factors can contribute to the final sound property of the guitar. As the primary source of sound radiation, the quality of the top is the most crucial part to determine the sound quality of the instrument. Over centuries of practices in making guitars, guitar makers have come up with some agreement in what materials should be used to construct the top. Two of the most common woods used to make guitar tops are spruce and cedar. Both of them have a high stiffness to density ratio, which makes them strong but also flexible. There are some manufacturers also using composite materials (mainly carbon

fiber), such as Martin and Ovation. However, based on French's [12] description, even the some composite materials have a very high stiffness-density ratio, both guitar makers and players still love using natural wood as the main construction material.

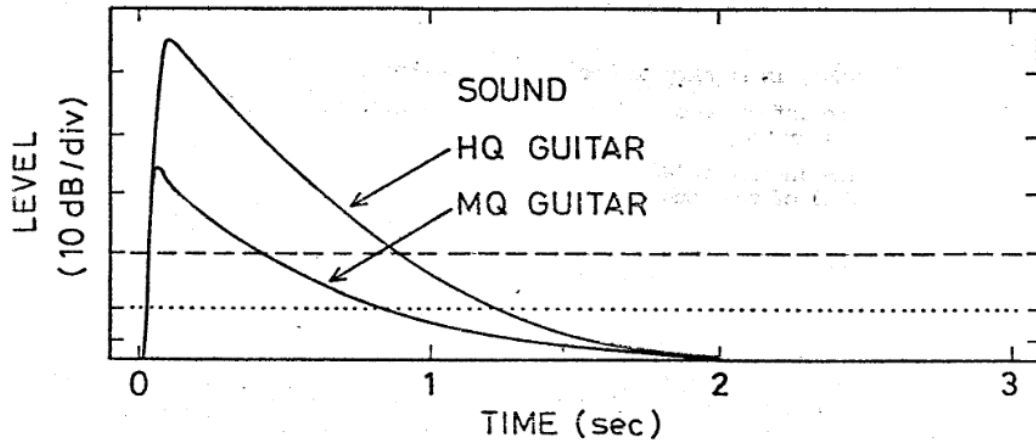


Figure 1.3 Comparison of the initial decay between a high quality and low-quality guitar (Source: Caldersmith [3])

Table 1.1 Stiffness to density ratio of materials used to make acoustic guitar tops

Material	Young's Modulus/Specific Gravity (GPa)
Sitka Spruce	27.5
Engelmann Spruce	26.8
Red Cedar	24.1
Carbon Fiber	93

Under the top are the bracing sticks (Figure 1.4). The original purpose of adding bracing was to support the top to prevent bending deflections from the tensions of the strings. However, guitar maker also found that the bracing can significantly change the sound quality of the guitar. The presence of bracing will add additional weight to the top and also suppress some of the vibration modes, which could alter the frequency response of the guitar.



**Figure 1.4 Bracing on the back of the top plate (source: <http://mullinguitars.com>)**

Sali [21] proposed a method to adjust the performance of the guitar by adding weight on the guitar top at various locations. This treatment is equivalent to modifying the bracing patterns of the guitar top. However, this method is still very experimental, and it also didn't provide a general solution to optimizing the guitar performance. This is why a simple and accurate measurement method can significantly help guitar maker to obtain the detailed information about the guitar dynamics and make quick adjustments. In bracing design, luthiers mainly need to achieve two goals. One goal is to not over-suppress the vibration of the guitar top, so some of the bracing sticks need to be placed on those nodal lines. Another objective is to balance the tone or to ensure there is no excessive power concentrated in certain frequency bands.

In addition to the bracing patterns, the shape of the brace could also potentially alter the dynamics of the guitar [7]. One of the most common treatments for shaping brace sticks is tapering its tip to reduce the weight added to the guitar top. Because the strength of the

top plate will become stronger when approaching to the top-sides joint, therefore trimming the bracing stick can both maintain the integrity and response of the guitar top. Another common practice is to make the scalloped bracings [7] (Figure 1.5). This technique has been applied to many high-quality guitars. However, the scientific explanation has been rarely touched. One of the reasons is because the complexity involved in the computational modeling.



**Figure 1.5. Shape of a scalloped bracing (Source: Dumond [7])**

In addition to the top materials, the bridge also plays a significant role in transmitting the string vibration energy to the top. The presence of the bridge, like the bracing, tends to add additional constraints on the top plate vibration [23]. Thus, its overall stiffness should be considered in the top design, where an excessive stiff bridge should be avoided.

Many studies were focusing on analyzing the first two modes of the guitar. Some other studies, for example, Boullosa [1] dedicated to studying the vibration of classical guitar on higher frequency ranges. There are significant difficulties in measuring the high-frequency response. One is that the higher frequencies band tend to decay faster than lower modes, so in free-field measurement, these high-frequency powers may not be able to be picked by the microphone. Another factor is the presence of high-frequency noise. In Boullosa's study, collected time domain signal showed a significant background noise. To minimize the background noise, a semi or fully anechoic chamber is preferred. There are different ways to measure the vibro-acoustic properties of the guitar. Such as putting



accelerometers on the guitar top, using a microphone to pick up the radiated sound or use hologram technique to observe the motion of the guitar ([1][6][14]).

The impact hammer plus microphone configuration is commonly seen in the literature ([6], [20]). One of the merits of this method is that it can measure the radiated sound directly from the guitar rather than the vibrations of the top measured by accelerometers. Moreover, for some special cases, such as measuring the near-field low-frequency response, it is not necessary to have a quiet environment for the test (Figure 1.6).

Some tests were conducted using the transducer to measure the vibration at the bridge as the input and measure the sound pressure [15][10]. The result from this measurement could tell the sound radiation efficiency of the guitar, which indicates how much vibration energy could be converted into acoustic energy. In Lai's measurement, the radiation efficiency was measured by placing microphone 10mm away from the guitar top. The radiation efficiency of the first two resonances was measured about 0.4.

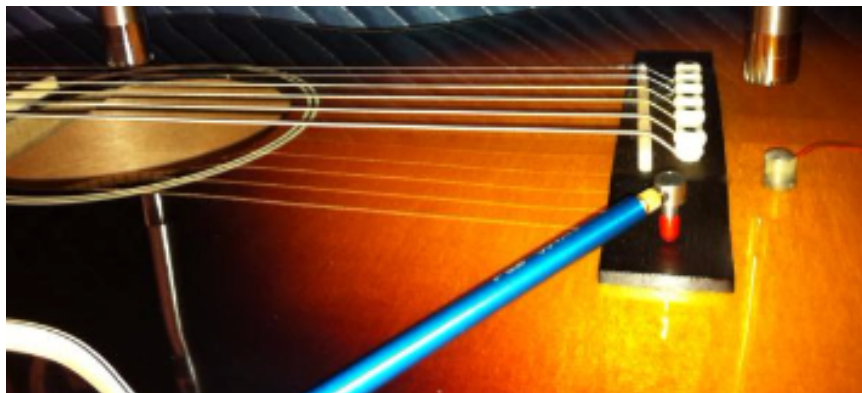


**Figure 1.6 Near-field measurement for the guitar FRF (Source: Hess [6])**

Some researchers looked at the mode shape the guitar top using Chladni patterns [5][9]. In this method, oscillating forces with different frequencies are generated and applied to the guitar body (shaker or speaker). We could see the nodal lines by placing loose sand particles on the top of the guitar board. This experiment could help luthier to distinguish

the vibration mode and help them to modify the bracing design to enhance the dynamics of the instrument.

Figure 1.7 illustrates this methodology, where the Chladni pattern could be clear seen on the top. The complicity of the pattern also increases with the rise of the oscillating frequency, which will induce higher modes on the top to produce more nodal lines.

All testing method described above need the physical contact with the guitar, which is not appropriate for valuable instruments. The contact method will either adding mass to the guitar body (transducers) or potentially damaged the body (hammer strike). It is desirable to have some non-contact measurement technologies to test the guitar dynamics.

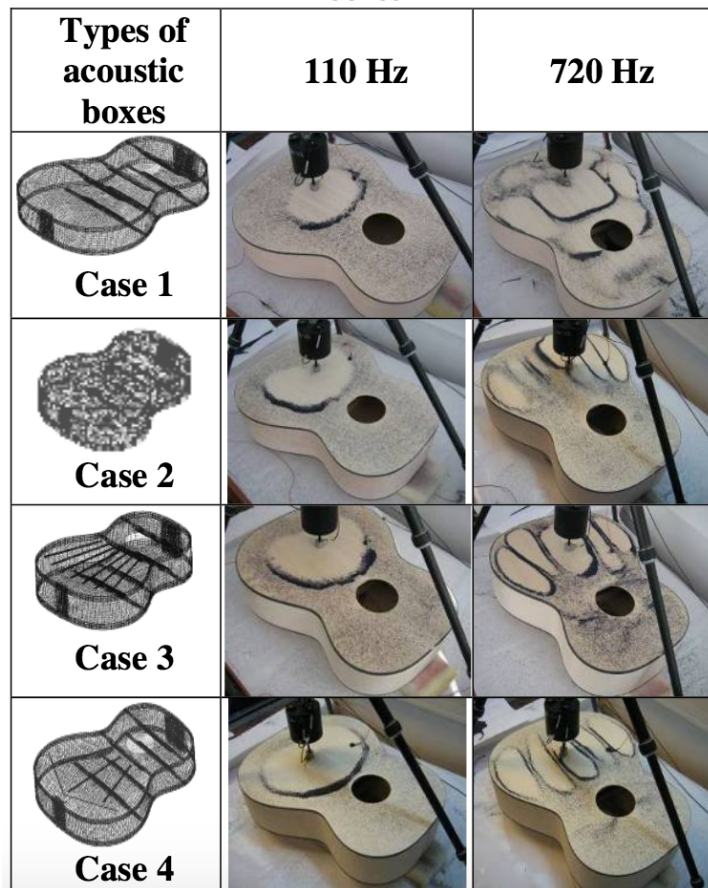


Figure 1.7: Mode shapes from applying oscillating forces with different frequencies (Source: Cutur and Stanciu [10])

Huber [13] proposed a method which introducing ultrasound force to excite the guitar top and using laser vibrometer to detect the vibrations. The basic theory of this method is that an audio resonance could be generated by combining two ultrasonic frequencies, and it could be used to excite the guitar. Compared to the speaker driven method, ultrasound force provides a good precision on the excitation locations, usually with a deviation less than 2mm. A comparison between conventional shaker-driven and ultrasonic force-driven method is showed in Figure 1.8. We can tell that the ultrasound force method can pick up the lower mode accurately but not having good performance at higher frequencies.

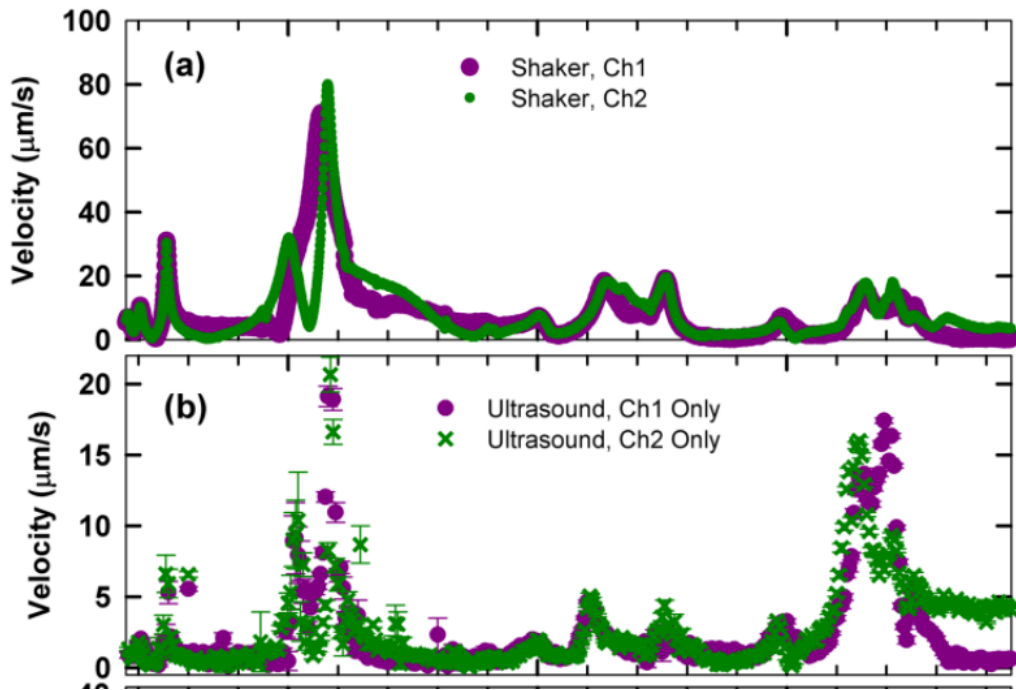


Figure 1.8 Comparison between contact method and ultrasound excitation method (Source: Huber [12])

With the considerations and lessons learned from previous studies, we decided to prepare a quiet chamber room for the testing. The methodology applied in measurement task was selected as the impact hammer-microphone system. Because the cost is relatively small

compared with the ultrasonic method and there is no significant noise as the shaker would introduce. The guitar top was assembled by us, where Collings Guitar from Texas provided the material. A fully constructed guitar (Yamaha FG-710) was also tested to investigate the effect of the body. Parameters such as microphone locations, effect of the soundhole, back and strings were also studied.

## Chapter 2.1 Fundamental Concepts in Acoustics and Vibrations

As we mentioned in the introduction, the mechanism that guitar can generate sound is the energy transmission from the vibrating string to the guitar body. The physics of a vibrating string is fairly easy to understand, which could be modeled by the one-dimensional wave equation

$$\frac{\partial^2 u}{\partial t^2} = a^2 \frac{\partial^2 u}{\partial x^2}$$

where  $u$  is the vertical displacement of the vibrating string and  $a^2$  is the ratio between the tension and the density per unit length. The solution of this governing equation could be found on many partial differential equation textbooks.

The vibrating string feeds the energy to the body and the body start to vibrate. Unlike in the one-dimensional case, the body vibration is essentially two dimensional, which could be treated as the vibration of plates. The biggest difference between string vibration and plate vibration is that the plate will not have a dominant resonance frequency as the strings. This is why string instruments tend to generate distinct pitches after the excitation, whereas percussion instruments could not.

Because of plates have larger contact areas and a rather even response over a wide frequency ranges, it is ideal to use it to amplify the sound resulted from given string vibrations. Also, because the nature of plate vibration, it will have much faster decay rate comparing with the string, so that it lead to a clear projection of the sound. Following sections will briefly introduce the physical model of plate vibration and its acoustic significance.

## Vibration of the plate

The top plate of the guitar is one of the main sources for sound generation [12][19]. The string vibration directly drives it and stirring the surrounding air to radiate sound. Therefore to understand the mechanics of the guitar, a good start point would be to understand the basic behavior of a vibrating plate.

The vibrational behavior of an isotropic plate with small deformation [16] could be modeled by the classical partial differential equation, which is

$$D\nabla^4 y + \rho \frac{\partial^2 y}{\partial t^2} = 0$$

where D is the rigidity of the plate as

$$D = \frac{Eh^3}{12(1-\nu)}$$

And E is the Young's modulus, h is the plate thickness and is  $\nu$  the Poisson's ratio and  $\rho$  is the density of the material. The displacement y in here will be complex (oscillating) to represent the actual behavior of the vibrating plate. And  $x_i$  are the spatial variable of the displacement (x,y,z, for Cartesian coordinate; r ,  $\theta$  for polar coordinate). The value zero at the right-hand side indicates this is a free vibration situation.

Based on the description in Leissa's [16] Vibration of Plates manual, the steady state solution for a free vibration plate with uniform boundary condition was assumed to be

$$y = A(x_i)e^{j\omega t}$$

Where A represents the displacement in the spatial coordinate ( $x_i$ ). By applying this solution, the fourth order differential equation could be decomposed into the product of two second order differential equations.

$$(\nabla^2 + k^2)(\nabla^2 - k^2)A = 0$$

Where k is defined as

$$k_n^4 = \frac{\rho\omega_n^2}{D}$$

If we treat the vibration area as a circular plane (area below the sound hole on the guitar top) with fixed boundary conditions, then it will have the form of well-known Bessel's functions [20]. Moreover, the solution to this governing equation is

$$y = [A_n J_n(k_n r) + B_n I_n(k_n r)] \cos(n\theta) e^{j\omega_n t}$$

where  $J_n$  and  $I_n$  are Bessel's function of the first kind and modified Bessel's function of the first kind of the  $n^{\text{th}}$  order.

The solution of the Bessel's function could provide information about the mode shapes and corresponding resonance frequencies of the vibrating plate, where the solution for an  $n^{\text{th}}$  order of the function will be the nodal diameters and its root will become the nodal circles. The physical meaning of these nodal lines simply indicates that there is no vibration along the line.

Figure 2.1.1 and Figure 2.2.2 demonstrates this phenomenon that the actual vibration behavior of the circular plate will be the combination of all possible modes. However, it is not an easy task to implement this model to simulate the modal behaviors of a real guitar top or even a circular shape wood plate. The difficulty mainly is from the non-homogenous distribution of the mechanical properties of the wood (recall these property terms in the governing equation) and the geometry of the instrument. Therefore only numerical methods could be used for modeling the behavior of the guitar. A basic setup in these numerical modeling is that we need to divide a complicated geometry into small elements with simple geometry, and then we assign mechanical properties to these

elements and define their boundary conditions. In this case, we will have a system of equations to solve, where the dynamics of every element will be influenced by adjacent elements, and the final solution should satisfy all these governing equations.

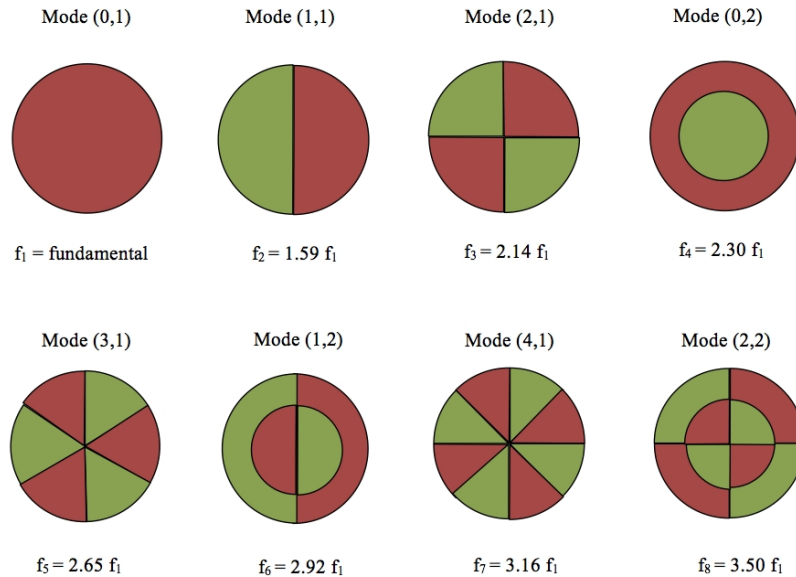


Figure 2.1.1 Mode shape with nodal circles and nodal diameters ([https://soundphysics.ius.edu/?page\\_id=1150](https://soundphysics.ius.edu/?page_id=1150))

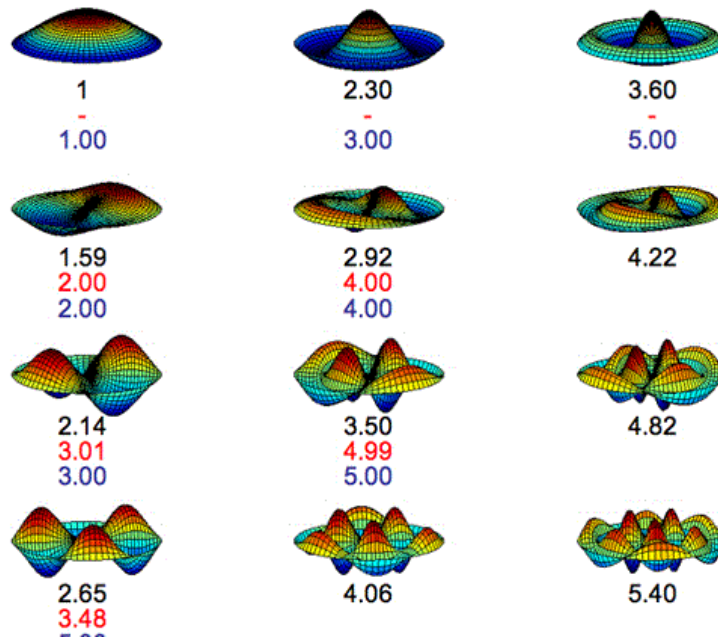


Figure 2.1.2 Vibration of plate from numerical simulation (black: drumhead, red: kettle drum, blue: tapla) (source: <https://plus.maths.org/>)



## Sound in fluid

The vibrating plate will not generate sound if it is placed in a vacuum space. The generation of sound is the fact that the disturbing medium that vibrates with time and travel in space. Therefore, the interaction between the vibrating source and the surrounding medium plays the most crucial role in the sound generation of musical instruments.

The mechanism of generating audible sound is that the oscillating pressure change within the air drives our eardrum, which will vibrate like a membrane so that our nerve system can perceive the sound. The equation of state of the gas indicates that the pressure change in a control volume of gas will also lead to a change in its density and temperature. However, the thermal effect of a sound field could be neglected to compare with the change of the density [8]. The dynamic process of a sound field, therefore, is modeled as an adiabatic process, which states that the change of the density of the air mainly relates to the change of its pressure with a small temperature variation. One fact should be noted here is that on a bigger scale, the change in pressure and density is a non-linear relation, which is governed by

$$P = \alpha \rho^\gamma$$

where  $\alpha$  is a constant and  $\gamma$  is the ratio between the specific heat of constant pressure and constant volume.

However in a sound field, the pressure disturbances resulted from sound wave are so small that the nonlinear effect could be ignored. Fahy [8] demonstrated the derivation of the wave equation, where the change of pressure could be expressed as

$$dP = -(\gamma P_0)(dV/V_0)$$

Where  $P_0$  and  $V_0$  are pressure and volume at equilibrium state.

The change of the density could be expressed in term of the volumetric strain, which is

$$d\rho = -\rho_0(dV/V_0)$$

The negative sign indicates that a positive change in the volume will lead a decrease in both the pressure and the density, so that

$$dP/P_0 = \gamma d\rho/\rho_0$$

If we assume the density in the system is  $\rho_0 + \rho'$ , which represents the summation of equilibrium density and deviation, then from the continuity equation we will have

$$\frac{\partial(\rho + \rho_0)}{\partial t} = -\frac{\partial u(\rho + \rho_0)}{\partial x}$$

where is  $u$  the particle velocity and  $x$  is the direction of the sound wave motion. So we will have

$$\frac{\partial \rho}{\partial t} = -\frac{\rho_0 \partial u}{\partial x} - \frac{\partial(\rho u)}{\partial x}$$

If we assume the mass flux  $\rho u$  is constant everywhere in the system, then we left with

$$\partial \rho / \partial t = -\rho_0 (\partial u / \partial x)$$

Moreover, through the relation between pressure and density, we can also have

$$\partial p / \partial t = -\gamma P_0 (\partial u / \partial x)$$

These relations are a mathematical demonstration of the mass conservation law, which states that the change of density in a fixed control volume will equal the difference between the fluid flows into the control volume, and it flows out of the control volume.

To understand the dynamics of the sound wave, we need to apply the Newton's second law of motion to link the pressure force and the wave motion, which is

$$\rho_0 (\partial u / \partial t) = -\partial p / \partial x$$

One assumption here is that the transporting medium is in static condition so that there is no acceleration from the fluid convection. This expression states that the change of particle velocity in a sound wave results from the pressure gradient, and the negative sign indicates all particles will flow from high pressure to low pressure.

By taking derivatives with respect  $t$  and  $x$  for last two equations, we have

$$\gamma P_0 \frac{\partial^2 u}{\partial t \partial x} = - \frac{\partial^2 p}{\partial t^2}$$

$$\rho_0 \frac{\partial^2 u}{\partial t \partial x} = - \frac{\partial^2 p}{\partial x^2}$$

which finally give us the one-dimensional wave equation

$$\frac{\partial^2 p}{\partial t^2} = c^2 \frac{\partial^2 p}{\partial x^2}$$

where  $c$  is the speed of the sound wave in an ideal gas medium, which equals  $\sqrt{\gamma P_0 / \rho_0}$  or  $\sqrt{\gamma R T_0}$ .

Similar to the one-dimensional wave equation, solution of this wave equation will give the information about both the spatial and time variations of a particular sound wave, and any sound wave could be expressed as a linear combination of different sound waves.

Because of the vibrational nature, acoustic pressure is a complex value, and it could be related to the flux of the fluid particle by

$$u = p/z$$

Olson's [19] book has a detailed description regarding this process. In above equation  $z$  is the acoustic impedance as

$$z = r + j\omega M - \frac{j}{\omega C}$$

Where  $r$  is the system resistance that evaluates how much energy will dissipate.  $M$  is the inertance of the system with the unit of mass divided by area and  $C$  is the acoustic capacitance of the system, which indicates the capability to store potential energy (reciprocal of the spring coefficient). The imaginary part of the impedance will give the inertial loss, which is due to the unsynchronized motion between the driving force and system reactions.  $\omega$  indicates the resonance frequency of the system. Through some combinations of the mass and stiffness, we are able to obtain the impedance without the imaginary part. In that case, the driving force and the motion of the system will move in phase and radiate the sound at this frequency. This natural resonance frequency could be evaluate by

$$\omega = 1/\sqrt{MC}$$

The simplest model to demonstrate the resonance of an acoustic system is the so-called Helmholtz resonator, which is mainly an enclosed container with a small aperture. The assumption of an effective Helmholtz resonator is that its dimension should be smaller enough compared with the wavelength of the interested frequencies [Kinsler 14]. By introducing airflow around the aperture, the exchange between the air in the body and the free air will occur and at certain frequencies, which is determined by the resonator dimension, resonance will happen. At resonance, the driving pressure will be amplified, and this phenomenon could be easily demonstrated by blowing a beer bottle. The resonance frequency of this resonator could be changed by putting different amount of liquid in the container since it can alter the capacitance of the container.

The Helmholtz effect is another primary source of the sound radiation of a guitar [10]. The sound hole will behave like the aperture of the Helmholtz resonator. The string

vibration will drive the air to flow around the soundhole which could potentially induce the resonance frequency of the guitar. Also, the plate vibration will change the volume inside the guitar body which will change the resonance frequency of the system. Thus, the guitar will behave as a coupled mechanical system, which could not be modeled as a simple combination of a vibrating plate and a Helmholtz resonator. The detailed description of this model will be introduced in next chapter.

### **Source of the acoustic wave**

If we consider the acoustic source as a single point in free space, then its radiation area would be a sphere where the sound power per unit area is defined as

$$I = \frac{P}{4\pi r^2}$$

The sound power per unit area is called the acoustic intensity. The acoustic power and intensity are usually calculated as dBs,

$$SWL = 10\log_{10}(P/P_0)$$

which is the sound power level,  $P_0$  is called the reference power level has value  $10^{-12}$  watt and

$$SIL = 10\log_{10}(I/I_0)$$

is the sound intensity level, where the reference intensity level is  $10^{-12}$  watt/m<sup>2</sup>.

As the sound intensity defined as

$$I = pu$$

Where  $p$  is the sound pressure and  $u$  is the fluid particle velocity. Recall that the particle speed of the fluid is defined as sound pressure divided by the impedance, therefore

$$I = p^2/z$$

so that the sound pressure level could be evaluated as

$$SPL = 10\log(p^2/p_0^2) = 20\log(p/p_0)$$

In the data acquisition task, the microphone will pick up the signal that represents sound pressure level. We can use this data to calculate the sound power spectrum from using the FFT so that we could know the distribution of the acoustic energy in the frequency domain.

The acoustic energy generated by an excited guitar will have different effects on the surrounding air based on the distance from the source. Close to the source is called the near field, where the air body will vibrate in phase with the source. One character of near field effect is that the amplitude of the vibration is not linearly related to the distance from the source. Beyond near field, the sound intensity will reduce linearly with the distance. In a free field, the radiated energy from the source will spread out over larger surface areas as the distance increases.

The boundary between near field and far field could not be clearly defined, the transition gradually occurs as the distance increase. If the source is a point source, the boundary of to the far-field should be at least two times of the wavelength of given frequency (<http://www.acoustic-glossary.co.uk/sound-fields.htm>) , and the wavelength is defined as

$$\lambda = \frac{c}{f}$$

That c is the sound speed and f is the frequency. The region of near-field will decrease as the frequency increases.

If the sound source could not be modeled as a point source, then the distance to the far field should be much larger than the dimension of the sound source.

## Chapter 2.2 Modeling Guitar as a Coupled Mechanical System

String instruments, like guitar and violin, usually have an enclosed body with sound holes on the soundboard. This body configuration will change the boundary condition for each component and also add additional impacts to the system. Therefore, the response of an instrument is no longer a simple combination of those individual responses. Many previous studies have agreed that the guitar is a coupled system, where the change of one component could also affect others.

One of the earliest physical models was proposed by Caldersmith [3], who described the guitar as a reflex enclosure. In this model, the back and sides of the guitar were assumed to be rigid where only the lower part of the top plate will vibrate (Figure 2.2.1). Based on their experimental result from the vibration holograms, this model proposed that the vibration area of the top plate would be circular with a fixed boundary.

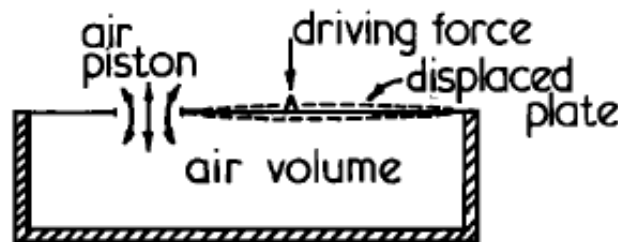


Figure 2.2.1 Guitar as a reflex enclosure (Source: Caldersmith [3])

The solution to this model is to solve the established Newtonian equation of motion, which for the plate motion is written as

$$\rho t \frac{d^2 x}{dt^2} = F - Dx + \Delta p$$

The left-hand side is the acceleration term, which includes the density ( $\rho$ ), thickness ( $t$ ) and the right-hand side is the summation of all effective forces, which include the driving

force (F in Pa), restoring force (D is the stiffness and x is the displacement) and the pressure force resulted from the pressure difference at the top and below the top plate ( $\Delta p$ ). In this model, the driving force was said to be complex, which is in order to simulate the force from the vibrating string.

The equation for the air-motion could be written as

$$M \frac{d^2 x}{dt^2} = p A_h - R \frac{dx}{dt}$$

Where M is the mass of the flowing air, p is the pressure in the guitar body,  $A_h$  is the area of the soundhole and R represents the resistance and radiation loss of the air motion.

These two governing equations show that the pressure couples this dynamical system. As we mentioned that in audio acoustics the thermal effect could be ignored, and the pressure change will have a linear relationship with the volume change (adiabatic), that is

$$dP = -(\gamma P_0)(dV/V_0)$$

Moreover, in this model, the total flow volume of the system will be the air displacement from both the soundhole and the plate, which could be expressed as

$$\delta V = x_p \int A_p + x_h \int A_h$$

Therefore, the pressure force in the governing equation could also be a function of the displacement from both the plate and soundhole air motion. The detailed solution of this model could be found in the paper (Caldersmith[3]).

There are two fundamental modes could be derived from this system, and they occur when the air-volume restoring force become zero. The first mode is the fundamental mode of the airflow, where the plate and soundhole airflow moving in antiphase or the guitar is breathing at this mode. However, this model may not be sufficient to explain the



second resonance mode, which also requires a minimum air restoring force. The proper explanation was addressed by other studies that the back of guitar should not be modeled as a rigid part. The reason is that if the back is also moving, then at some point it will move in phase with the top, so the air pressure in the body will be stable.

A graphical representation of the first two modes is shown in Figure 2.2.2. The first mode is the effect of a Helmholtz resonator (Soundhole mode), except the body is not rigid. A net air flow from the sound hole is dominating due to the volume change inside the guitar body where the top and back are moving in opposite directions. In the second mode (plate or body mode), the top-back plates are nearly moving in the same direction so that the airflow through the soundhole will be significantly smaller than the first mode. In both cases, the air pressure in the body will be stable so that the air-volume restoring force will be their minimum values.

Another mechanical model for this coupled system is demonstrated in Figure 2.2.3 (Christensen [4]). In this model, the guitar's back and sides are also assumed to be rigid. The motion area of the top board is having area  $A$  and mass  $m_p$ , a spring is simulated under the top plate to represent its stiffness, which could be thought as the free boundary version of the previous model.

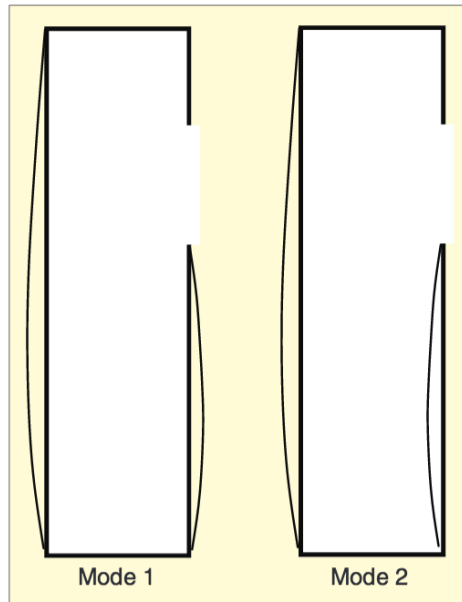


**Figure 2.2.2 First two mode of an acoustic guitar (Source: French [11])**

An oscillating force will be introduced from the string vibration, which will drive the top plate to vibrate. The sound hole is then modeled as a chunk of oscillating air mass ( $m_a$ ) that exchanges the air volume in the body with the free air. The friction term is also included in this model ( $R_p$ ) to represent the energy dissipation.

The governing equations are essentially the same as the previous model, which is written as

$$m_p x''_p = F - k_p x_p - R_p x'_p + A_p \Delta P$$

$$m_h x''_h = A_h \Delta P - R_h x'_h$$

Where  $R_h$  represents the resistance of the air.

Some key values were derived from these coupled differential equations, and they are listed in Table 2.2.1.

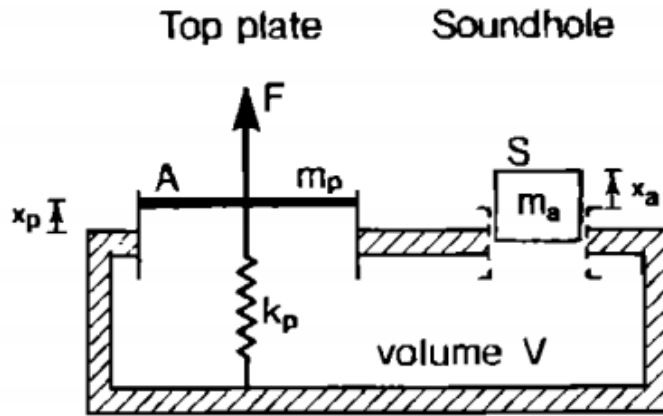


Figure 2.2.3. Two degree freedom system of a guitar model (Source: Christensen [2])

Based on this values, we can see that the coupled-breathing mode of the guitar is lower than the Helmholtz frequency and the coupled-plate mode is higher than actual plate resonance because

$$\omega_1^2 + \omega_2^2 = \omega_h^2 + \omega_p^2$$

Table 2.2.1 Important values for an air-body couple guitar model (= ratio between change in volume and pressure,  $k_p$ =stiffness of between the plate and the cavity)

Plate resonance frequency with no cavity ( $\omega_p$ )	$[(k_p + \mu A_p^2)/m_p]^{0.5}$
Plate resonance with no stiffness( $\omega_a$ )	$[\mu A_p^2/m_p]^{0.5}$
Helmholtz resonance frequency ( $\omega_h$ )	$[\mu A_h^2/m_h]^{0.5}$
Coupled frequency ( $\omega_{ph}$ )	$[\omega_h^2 \omega_a^2]^{0.25}$
Coupled first and second mode ( $\omega_1$ & $\omega_2$ )	$\frac{1}{2}(\omega_p^2 + \omega_h^2) \pm \frac{1}{2}[(\omega_p^2 - \omega_h^2)^2 + 4\omega_{ph}^4]^{0.5}$

A more complicated model is also presented in Christensen's [2] paper, where the motion equation of the back was added to the system. The effect of the back was compared with the rigid-body model, and the major impact was that the first plate mode was shifted, and an additional back-response mode could be seen as the third mode the guitar. The effect

of the back is shown in Figure 2.2.4, where the light curve is the model without the backplate motion, and the thick curve represent the model with the backplate. The result shows that if the resonance frequency of the back plate ( $F_B$ ) is in between the air mode and plate mode, then the actual body mode will be shifted toward to higher frequencies and vice versa.

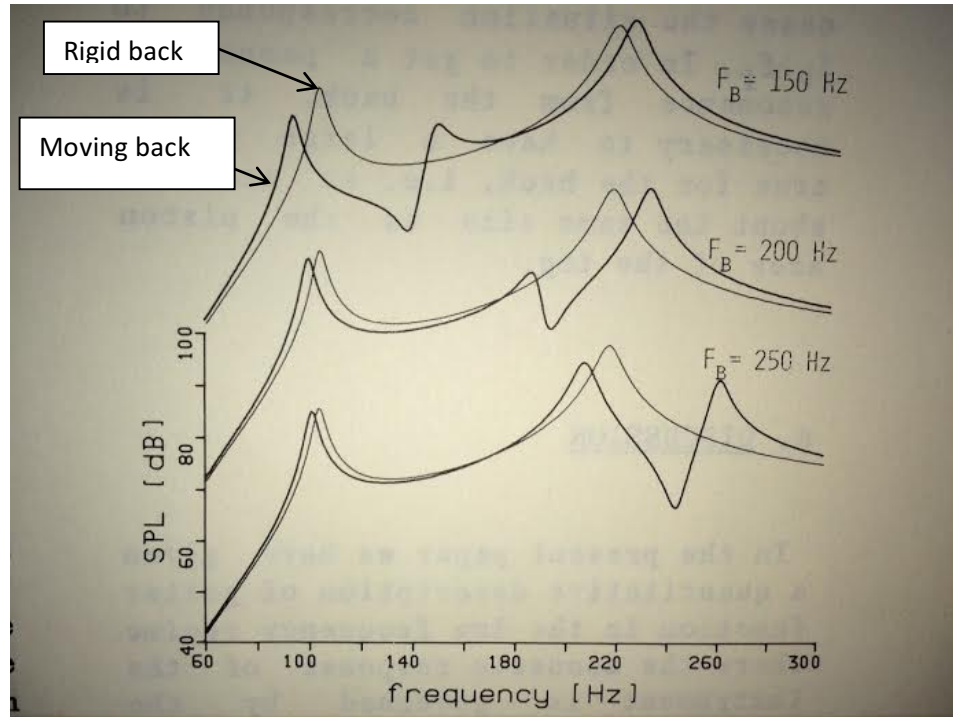


Figure 2.2.4 Effect of the back plate motion to guitar FRF (Source: Christensen [4])

Another way to think about the guitar is that it could be treated as a parallel circuit, where the mass, stiffness, and damping could all find their electrical counterparts in this circuit [9][10]. Figure 2.2.5 illustrates an equivalent circuit built to simulate the guitar. The parallel configuration indicates the coupled system of the guitar, which includes the plate mode and soundhole mode (rose). In this circuit diagram, after the excitation at the bridge, the current will firstly move through the series of inductance (mass), capacitance (stiffness) and resistance (resistance) of the top plate. After reached to the resonance frequency, it then goes through another inductance and resistance which represent the

radiated and dissipated energy. The motion of the top plate will also make the air in the body to oscillate ( $M_{AV}$ ) which will induce the air flow in and out of the soundhole (rose). This air flow ( $M_{AR}$  and  $R_{AR}$ ) will also radiate acoustic energy ( $R_{ARR}, M_{ARR}$ ) and feed the remaining energy back to the system together with the resistance ( $R_{AV}$ ) and capacitance ( $C_{AV}$ ) of the air in the body to maintain the vibration of the system until all energy radiated and dissipated.

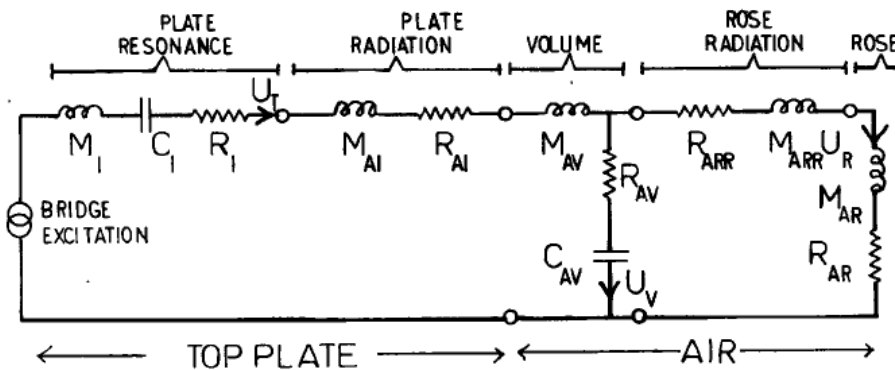


Figure 2.2.5 Equivalent circuit for an acoustic guitar (Source: Firth [4])

At lower modes, the soundhole and vibrating plate could be treated as a superimposed source because the corresponding wavelength is much larger than the distance between the two sources (Caldersmith [3]). However, the energy released from these two sources could be different. Research shows that the sound hole is the major energy source below 275 Hz, and the top plate starts to be dominant above this frequency (Strong [19]). The dominating power of the sound hole is also an indication of the important role of the back-plate, whose motion greatly enhanced the airflow through the soundhole.

At higher modes, the superimposed source model will not be valid because the guitar starts to behave as a dipole source. The coupling effect will intensify at higher modes, and it will lead to a more complicated response behavior over these modes, which is

represented by a higher modal density. Therefore, these simplified models mentioned above could only give confident results at lower modes.

In this section, we introduced some models proposed by prior studies to simulate the dynamics of the acoustic guitar. They all agreed with the coupling effect of the guitar, and all have some simplifications (rigid or flexible back). In our experiment, we expect to see this coupling effect in our data and explore its influence on the guitar frequency response.

## Chapter 3.1 Signal Processing Methodology

This section will describe the signal processing procedure for analyzing the frequency response function of the radiated sound from the hitting guitar top. The frequency response is defined as the ratio of the output Fourier transform to the input Fourier transform of the time domain signal [16]. The output signal is the sound pressure data acquired by the microphone, and the input is the force sensed by the impact hammer. Newton's Third Law states that any action force will have a reaction force with equal magnitude and opposite direction. Therefore, the force sensed by the hammer will be the force that hammer exerted to the guitar top.

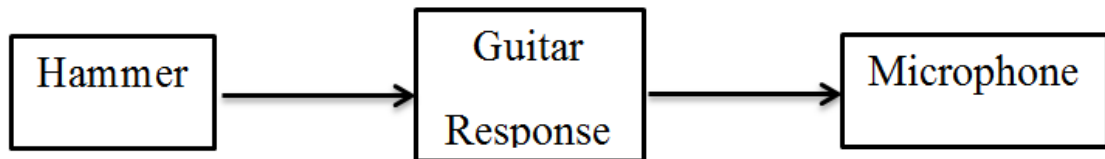


Figure 3.1.1 Block diagram of a measurement configuration

The first statement we need to make is that we will treat the guitar as a linear and time-invariant system that the magnitude of the microphone data will be proportional to the magnitude of the hammer force. Combined input signal will also result in a linearly combined output signal. The input-output relation (system response) will not change with time.

One assumption we made here is that we could treat the hammer strike as an impulse so that the sound generated by the guitar top will be the impulse response of the hammer strike. A mathematical explanation of this relation could be given using the convolution theory, where the output signal of an LTI system is obtained through

$$y(t) = \int_{-\infty}^{+\infty} x(\tau)h(t - \tau)d\tau$$

for continuous signal and

$$y[n] = \sum_{k=-\infty}^{k=+\infty} x[k]h[n - k]$$

for a discrete-time signal.  $y(t)$  and  $y[n]$  are the output signal of the system,  $x(t)$  and  $x[n]$  are the input signal and  $h(t)$  and  $h[n-k]$  are the impulse response.

An intuitive way to understand the signal convolution is that every output signal at time  $t$  is the linear combination of the instant response at  $t$  (or  $n$  in discrete time) and the responses (represent by  $\tau$  and  $k$ ) of all past input signals.

Figure 3.1.2 shows an exponentially decayed simple oscillator. The frequency of this oscillator is called the natural frequency of the system. The input signal is an impulse at time equal zero. Based on the fundamental signal theory, the output signal to an impulse will be the system impulse response. We could observe this phenomenon from Figure 3.1.2 where the impulse response (black curve) overlaps with the output signal (green curve).

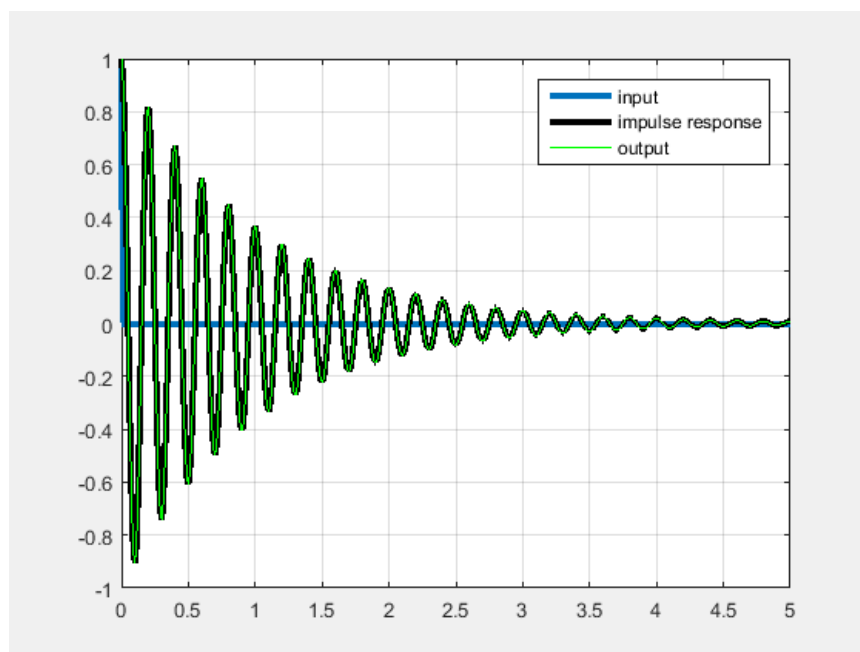


**Figure 3.1.2 Output signal to an impulse input**



However, the impulse response of a guitar could be hardly said only having one oscillating frequency. This phenomenon was explained by the modeling of a thin plate, which shows that the plate could have different vibrating modes and, therefore, having different oscillating frequencies. Figure 3.1.3 shows an impulse response function with more than one mode (10Hz, 15Hz, 20Hz, 50Hz, and 100Hz). For simplicity, their amplitudes are all assigned to be 1 and a damping coefficient of -1. We can indicate the linearity from the initial amplitude, where is the summation of five unit impulses.

Fortunately, the impulse response function of an LTI system will be the linear combination of all frequencies components. Moreover, this combined signal could be decomposed using the Fast Fourier Transform algorithm so that we could see the distribution of these modes in the frequency domain.

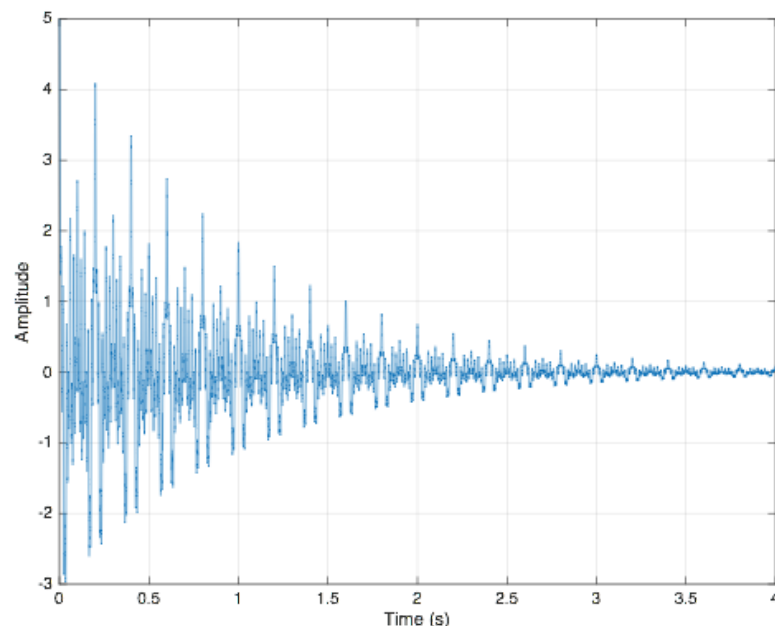


**Figure 3.1.3. Impulse response function having more than one frequency**

This frequency domain representation will indicate the magnitude of the response at different frequencies, thus give us an overall idea about the vibrating behavior of the

guitar top. Figure 3.1.4 shows the frequency domain information using the FFT to decompose the impulse response function represented in Figure 3.1.3. An interesting point could be observed is that the amplitudes on the frequency domain are not one, which is our original amplitude. The reason behind this power reduction is due to the damping of the signal. Recall the mathematical expression for a simple damped oscillator

$$x(t) = Ae^{-rt+j\omega t}$$

When we calculate the Fourier Transform the damping term  $e^{-rt}$  will be integrated, which will lead to the power reduction. If we get rid of the damping term, then the magnitude returned from the Fourier Transform will just be A, where the Fourier Transform for a continuous time signal is

$$X(j\omega) = \int_{-\infty}^{+\infty} x(t)e^{-j\omega t} dt$$

The damping will also affect the resonance frequency as well, which is related by

$$\omega_d^2 = \omega_0^2 - r^2$$

where  $\omega_d$  is the damped resonance frequency of the system.

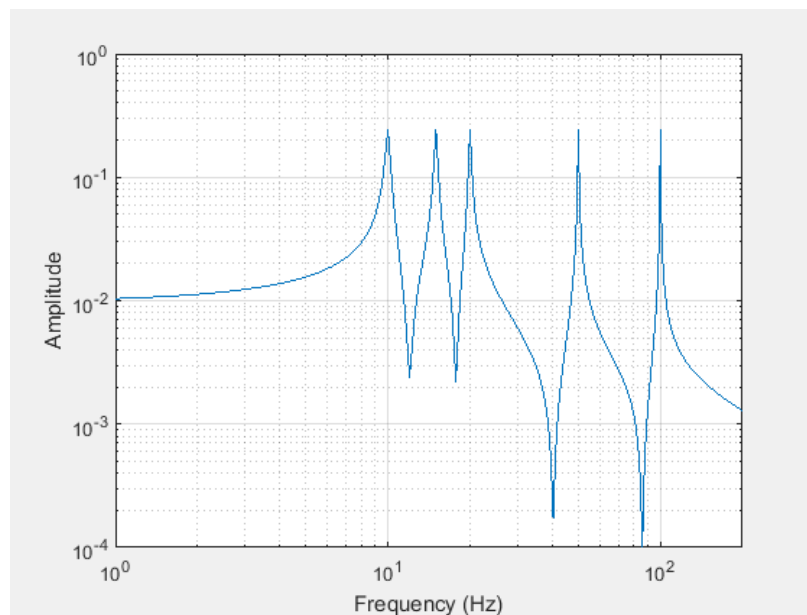


**Figure 3.1.4 Frequency domain representation of damped multi-modes signal**

As we demonstrated in Figure 3.1.4, a damped oscillator will lead to a wider peak on the spectrum. Therefore, not only the magnitude of the frequency response but also the shape of the response can represent the actual behavior of the signal. The shape of the of the frequency response could be interpreted by a parameter called the quality factor (or Q factor), which usually calculated as

$$Q = \frac{f_c}{\Delta f}$$

Where  $f_c$  is the center frequency of the resonance peak,  $\Delta f$  is the frequency band with an upper and lower limit. This frequency band is usually taken as the power at upper and lower limit drops to the half value of the center frequency.

The quality factor could also be expressed in term of

$$Q = \frac{\sqrt{mk}}{R}$$

that  $m$  is the mass;  $k$  is the spring stiffness, and  $R$  is the damping coefficient of the system from the differential form of the simple oscillator

$$m \frac{d^2x}{dt^2} + R \frac{dx}{dt} + kx = 0$$

Moreover, the previous expression could also be written in term of

$$Q = \frac{\omega_0}{2r}$$

where  $\omega_0$  is the resonance frequency and  $r$  is the exponential decay of the signal magnitude. Therefore, through evaluating the quality factor we can obtain a qualitative understanding about the system damping.

The transfer function of the frequency response is simply a ratio between the output Fourier transform and the input Fourier transform

$$H(f) = \frac{O(f)}{I(f)}$$

However, the input and output from the Fourier transform usually contain complex terms, which represents the phase effect. To make the division easier, we can multiply the equation by the complex conjugate of the input Fourier transform, which is

$$H(f) = \frac{O(f)I^*(f)}{I(f)I^*(f)}$$

and take the real part of the frequency response, which represents the magnitude of the response.

This section introduced the methodology in the signal processing part of this study. We will treat the guitar as an LTI system where the system response is affected by both the spectrum energy and damping rate. The hammer will introduce the input signal, and the microphone will pick up the output signal. The system response will be evaluated by dividing the spectrum of the output to the spectrum of the input. The system damping property could be either observed from the time domain data (decay rate) or the spectrum (shape of the resonance peaks).

## **Chapter 3.2 Experiment Preparation**

The guitar board tested in this study has a traditional dreadnought shape with an X-bracing pattern. This configuration was originally developed by Martin in early the 20th century. This type of body design was mainly applied to construct steel-string guitars. Compare to classical guitar, steel-string guitar requires the body, especially the guitar top to sustain much higher tension from the strings. Therefore, stronger support under the guitar top has to be deployed.

In the X-bracing (Figure 3.2.1), the X pattern in the middle and the two bars in the lower section are the main supports for the guitar top. However, it is not desirable to make the top too strong, which will suppress the response and reduce the overall sound radiation from the guitar. A compromise between the durability and flexibility has to be made to guarantee both the integrity and sound quality of the instrument.

This guitar top was made out of spruce. It is provided by Collings Guitars, which is a handcraft guitar manufacturer in Texas. The sample board has a small blemish at the lower part of the body (far away from the excitation point). However, there is no obvious discontinuity present on the board thus the effect of this small flaw was ignored in our analysis. The bracing sticks were deployed to the top board by using the double-side tapes and clamped for a period to consolidate the cohesion between the guitar top and the bracing sticks.



**Figure 3.2.1** Guitar board tested in this study



**Figure 3.2.2** Quiet chamber built for the frequency response measurement

To minimize the impact of the noise, a quiet chamber was constructed in the electronic music instrument lab at Tufts University (Figure 3.2.2). This chamber is about 6' tall, and its area is about 24 square feet. The wall of the chamber was covered with soundproof foams. Two thick wood doors filled with fiberglass were also constructed to prevent noises from outside. The floor of the chamber is covered with two layers of stock carpet. Both the testing rig and data acquisition device were placed on the sound-proof pad. The room response was tested by placing the microphone in the chamber and striking the hammer on a clay tablet outside the room so that the microphone will only pick up the background noise of the room.

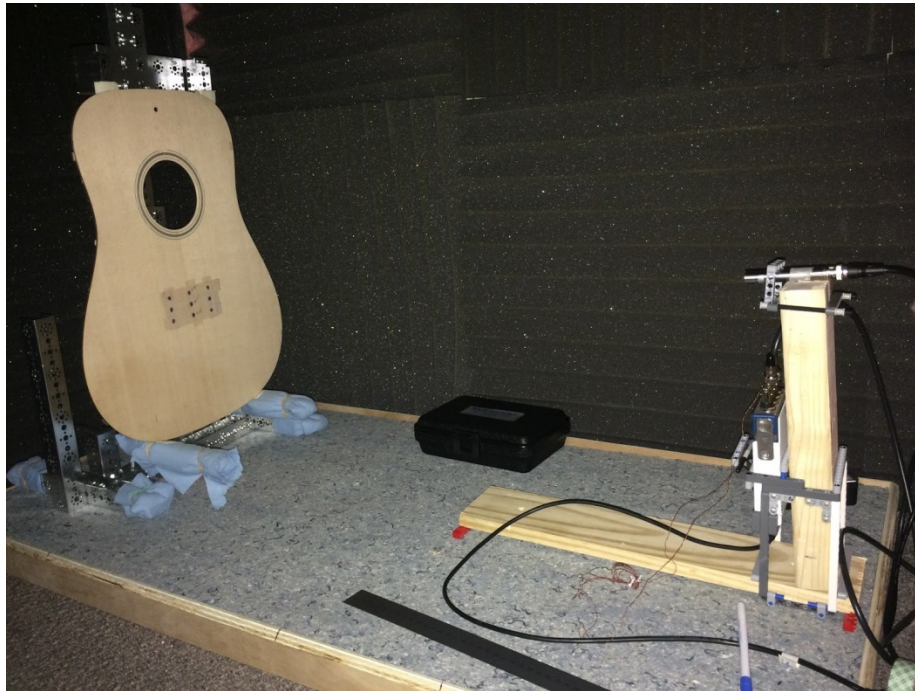
Testing apparatus used in this research are listed in Table 3.2.1

Table 3.2.1: List of test equipment

Input source	PCB impact hammer (model 086E80)
Output sensor	G.R.A.S. microphone (Type 46AE)
Data acquisition	NI 9234
Communication	NI USB-9162
Signal amplification	G.R.A.S. Type 12AL
Signal processing equipment	Dell PC (model Latitude 3440)
Signal processing software	Labview 2014 and Matlab R2015a

In the testing sessions, the soundboard will be simply supported on an aluminum rig. The surface area of the metal rig was minimized to eliminate unwanted sound reflections. The basic procedure for the data acquisition task is that by striking the surface of the soundboard, the microphone will pick up the radiated sound (by sampling rate 48 kHz), and then the data acquisition device will import the digitized sound information into the computer, and the available programs will analyze the signals. The experiment setup is

demonstrated in Figure 3.2.3. Identical equipment and methodology were used to measure the fully constructed guitar.



**Figure 3.2.3 Experiment setup**

Two Labview VIs were used to analyze the data; one is for real-time analysis that after each test, the corresponding frequency response function would be calculated. This VI also appends the raw data to .csv files, which will be analyzed by other VIs to calculate the averaged frequency response function for all instances. All FRF plots in Chapter 4 are the averaged result from each run, where each run takes 15 hits. This average FRF will be plotted together to see how the frequency response changes with the change of testing parameters (such as the distance from the microphone, the location of the striking point, and different body configurations).

In the test, both the hammer and microphone need couple minutes to stabilize. We used another Labview VI to keep monitoring the reading from both sources until they all settle down at zero magnitude. For the striking mechanism, at beginning we were thinking



using an automated device (small robot arm). However, by considering the associated noise, the guitar top will be simply hit by hand. The variation of the output will be normalized by the input.

## Chapter 4.1 Result

There are some requirements have to be satisfied with our data. One is that we expect the background noise will not distort our data, and the resonance peaks could be easily identified in the spectrum. The second requirement is that our data should be highly repeatable. Even though in the real world, every piece of wood has different properties, which make every instrument unique, the frequency response function from our test should be comparable with other studies.

Results from past studies showed that one of the main features of an X-braced steel string guitar was that it usually has two resonance peaks around 100Hz and 200Hz [4][10], which represent the breathing mode of the sound hole and the fundamental mode of the top plate. If we decouple the guitar frequency response, the first mode of the top board will shift to lower frequencies, which means the first peak we obtained from the guitar top's response function will be at lower frequencies compared with the result of the full guitar test.

One of the main interests in conducting this study was that we want to see the effect of the bracing to the top board. Theoretically, the presence of bracing will suppress some of the lower modes of the top board and, therefore, adding more weight to the higher mode response in the spectrum. The effect of the enclosed body to the guitar top will also be investigated to see how it will change the frequency response of the guitar top.

The first measurement we did was to characterizing the noise of the room. This task was accomplished by placing the microphone in the testing chamber, and then tapping the hard surface using the hammer outside the room. In this case, we could obtain the same input signal and the microphone in the chamber will only pick up the noise so that the

noise response could be evaluated. Figure 4.1.1 demonstrates the comparison of a typical guitar top response and the room noise response. The guitar response displayed in this figure was the averaged spectrum from 15 strikes, and all response plot showed in this chapter are averaged result. FRF below 150 Hz will be severely distorted by the room noise. Distinct response peaks could be observed on the guitar response curve from the first peak at 170 Hz to 7000 Hz. One thing should be mentioned here is that the increased room response at higher frequencies was not because of the acoustic energy, it was because of there was no significant amount of energy within these frequencies from the input so that the ratio between output and input became large.

Figure 4.1.2 shows the hammer power spectrum from different strikes. A significant drop occurred after 1000 Hz, and this effect will lead to an increase in the frequency response as mentioned earlier. The additional impact of this magnitude reduction could be the loss of repeatability of the data if the reduction rate in the frequency domain is different in every excitation. From Figure 4.1.1 we can see the separation of noise and signal is clear so that the background noise will not have an obvious impact on our signal.

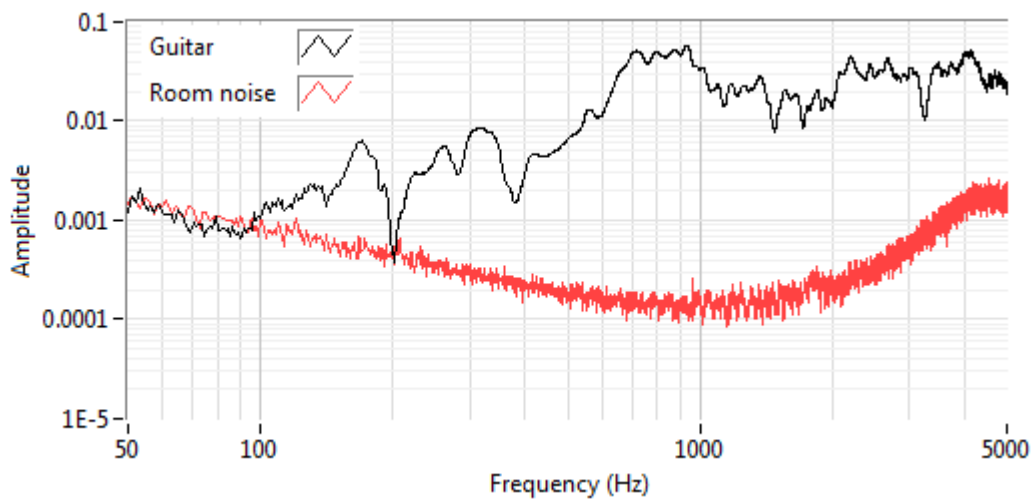


**Figure 4.1.1: Top plate response (Black) and room noise response (Red)**

To see the consistency of the top behavior, we conducted tests on different days over the testing period. Same test configuration was applied, which included the same bracing configuration, microphone location, and the excitation point.

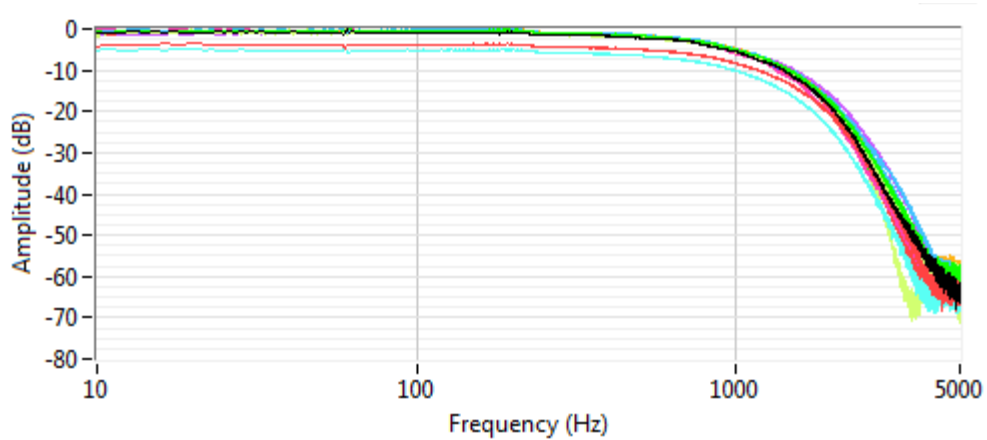


Figure 4.1.2 Hammer frequency response

Figure 4.1.3 demonstrated the frequency response function obtained from three different trials with same test configuration. The data was obtained from the test where the full bracing pattern was deployed, the microphone was pointed at the middle of the top, at 40 cm from the board and the excitation point in these tests was at the 6th string location within the bridge area (Figure 4.1.4). Moreover, additional testing parameters are listed in Table 4.1.1.

Table 4.1.1 Testing Parameters

<b>Testing Parameters</b>	Guitar response function
Microphone distance	
Source Location	
Sound hole	
Back configuration	
String Tension	

Our cutoff frequency, in this case, is from 50Hz to 5000 Hz. The data shows that the frequency responses from three tests almost overlap each other within the band from the first peak to 400Hz. From 400Hz to 1000Hz, the magnitude of the response start to deviate, but the quality consistency still could be observed. Above 1000 Hz, the frequency response lost the consistency, which is primarily because of the variations in magnitude reduction of the hammer response above 1000 Hz. Therefore, our focusing frequency range, in this case, will be between the first peak to 1000 Hz.

In Figure 4.1.3 we can observe the first peak is located around 173 Hz, which is the lowest resonance frequency in this configuration. This resonance frequency is different from the one obtained from the fully constructed guitar, which is possibly due to the coupling effect between the guitar top and the air in the guitar body that tend to shift the plate fundamental mode to higher frequencies. Another possibility could be the change of the boundary condition. Compare with the guitar, the tested guitar top was confined by four supporting points instead of a fully clamped boundary.

Another two peaks occur at 250 Hz and 310 Hz, which are the higher resonance modes of the top. A detailed modal analysis could be achieved by shaking the board with corresponding resonance frequencies and record the Chladni pattern to see the mode shapes. A flatter responses with higher magnitude were observed from 700 Hz to 1000 Hz; this occurrence is mostly due to the increase of the mode density, plus the response at higher frequencies usually decays faster, which could lead to a flat response in the spectrum. Significant variations from three measurements occurred at low frequency (<150 Hz) and higher modes (>500 Hz). We propose the variation below 150 Hz was

primarily from the background noise and higher mode variation was from the input variation as we mentioned earlier.

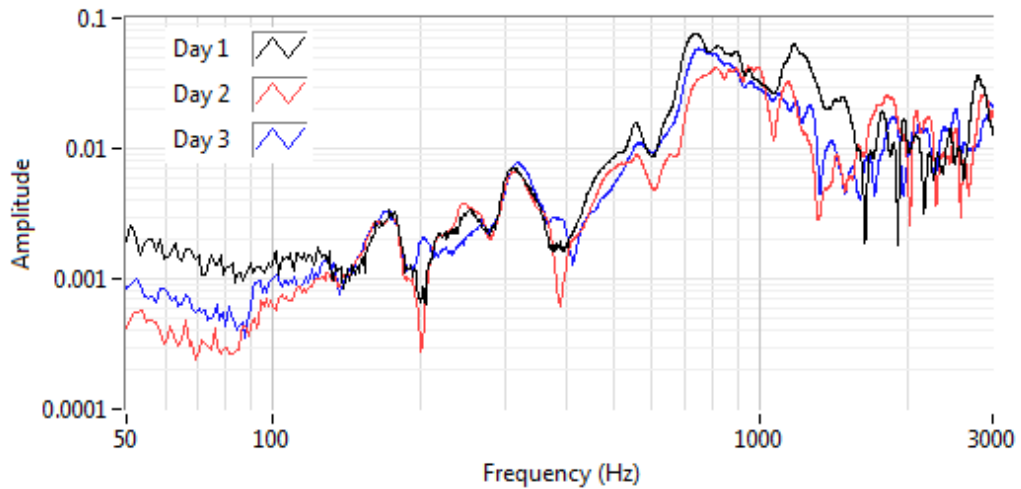


**Figure 4.1.3** Frequency response of guitar board at different times

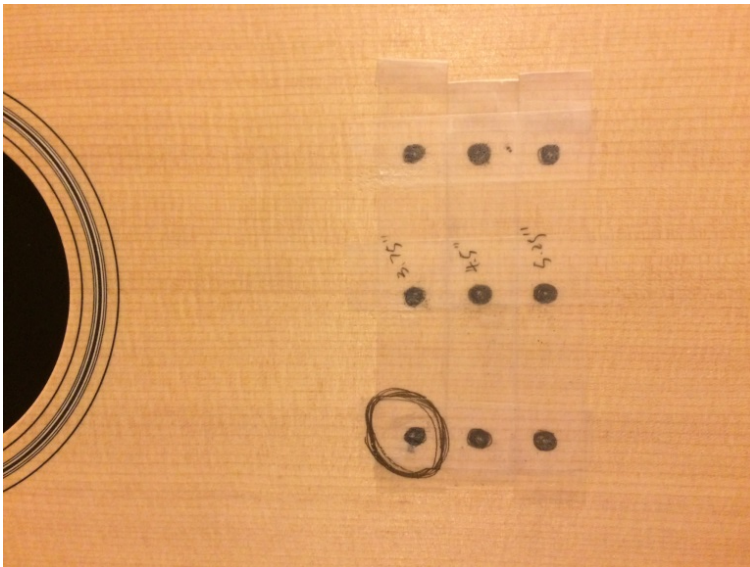


**Figure 4.1.4** Excitation location (circled)

Between these response peaks, some anti-resonances were also observed (200 Hz and 400 Hz). A potential reason for this phenomenon could be that the vibrations at these frequencies were suppressed by the bracing, and, therefore, it cannot induce corresponding sound radiation. To investigate the actual mechanism behind this power

reduction, we need to attach transducers on the top to measure its actual vibration modes, which we did not have in this research.

After testing the data repeatability, the influence from the microphone distance was investigated. The result from these tests could tell the effect of the near field and potentially give information about the transition to the free field. Three distances were tested, which were 40cm, 60cm, and 120cm. Figure 4.1.5 shows the result from these runs with the excitation point same as the result showed in Figure 4.1.3.

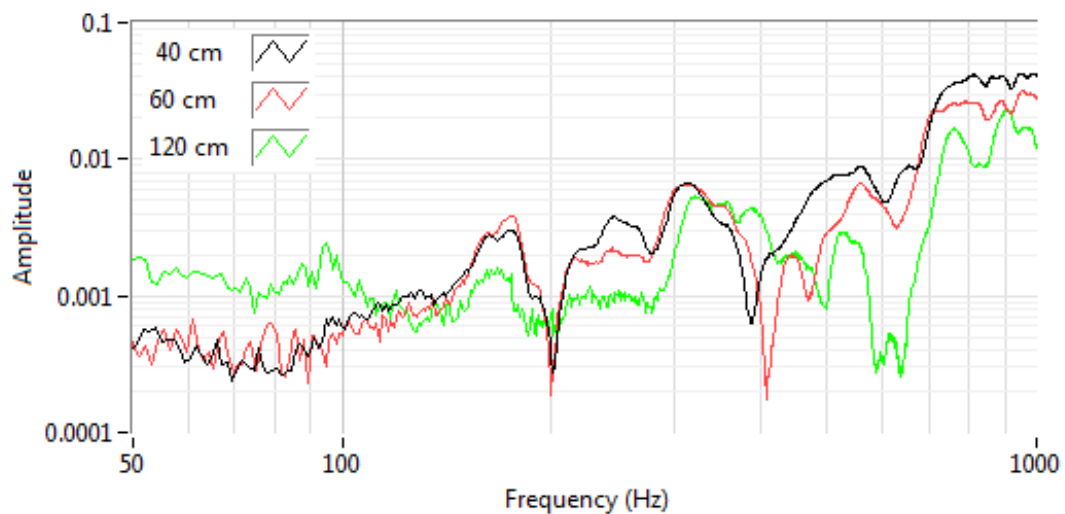


**Figure 4.1.5 Guitar top response picked up at different locations**

The first impression of this outcome is that there is hardly a clear relationship between these curves. However, we still can observe the first mode happens at all three curves. There is no obvious difference between the 40cm and 60cm cases, which is mostly because of the near field effect. The wavelength at this frequency is about 2m ( $340\text{m/s}$  divided by  $170\text{ Hz}$ ), which means to avoid near-field effect, the microphone should be placed at least 2m (usually two wavelengths away is recommended) away from the source. From 200 Hz 700 Hz, the effect of the distance could be hardly addressed, which again is because of the near field effect.

The response above 700 Hz, however, show a clear descending order as the pickup distance increase. The wavelength at 700 Hz is about 0.5 m, where the transitioning effect could be dominant. Another reason that could lead to this near-field effect is the dimension of the source. We could not treat the guitar top as a point source if we only place the microphone 0.5 m away from it. In addition, because the input response starts to deviate around 1000 Hz, accurate FRF become harder and harder to obtain.

Next, the effect of the bracing was investigated. The added bracing could generate additional nodal lines which could potentially suppress some the resonance modes. Figure 4.1.6 shows the FRF from three brace configurations. In the no-brace case, we would rather have a flat response around 170 Hz, which was the fundamental mode of the fully braced board. The added X-brace then suppressed this mode. However, one of the interesting results of this test was that the response at 170 Hz reappeared after applied the full brace.

One of the significant effects from the fully braced case was that it dramatically suppressed several modes, such as mode at 200 Hz and 400 Hz. At higher frequencies (above 1000Hz), the unbraced board would have several distinct peaks. Those peaks are not desirable for a musical instrument, which often require a rather flat response to deliver a balanced tone. A direct consequence from these peaks would be that the volume of the instrument will have significant variations when playing different notes. By adding bracings, the response at high frequencies became smoother compared with the unbraced board, which is usually a good sign for a musical instrument (Figure 4.1.7).



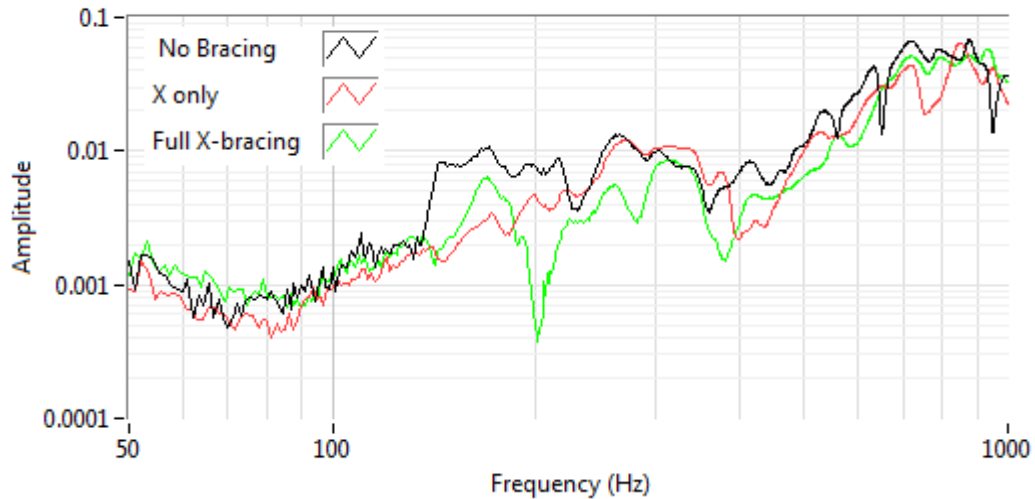


**Figure 4.1.6 FRF from different brace configurations (50 Hz -1000 Hz)**

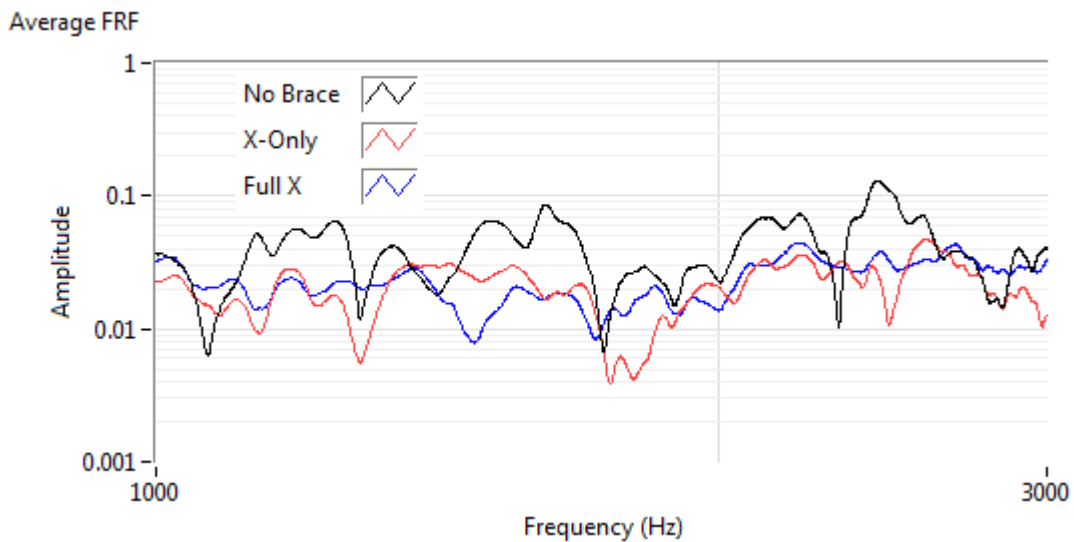


**Figure 4.1.7 FRF from different brace configurations (1000Hz -3000Hz)**

In addition to solely testing the board, a fully constructed guitar (Yamaha FG-710, and it will be referred as the “guitar” in later texts) was also tested to obtain its characteristics. A guitar tends to have a significantly different frequency response comparing with the board. The first change is the boundary conditions. In our previous test, the boundary condition of the naked guitar top was somewhere between a simply supported and clamped situation. However for the guitar case, it is mostly a clamped condition, which will lead to a different solution of the governing equations.

The added enclosed body will also play a significant role in shaping the frequency response, where the air in the body will interact with the vibration of the plate through the soundhole. As mentioned in the literature review, an additional mode will present in the frequency response function comparing with the naked guitar top case, which is called the breathing mode and it is the first peak in the FRF.

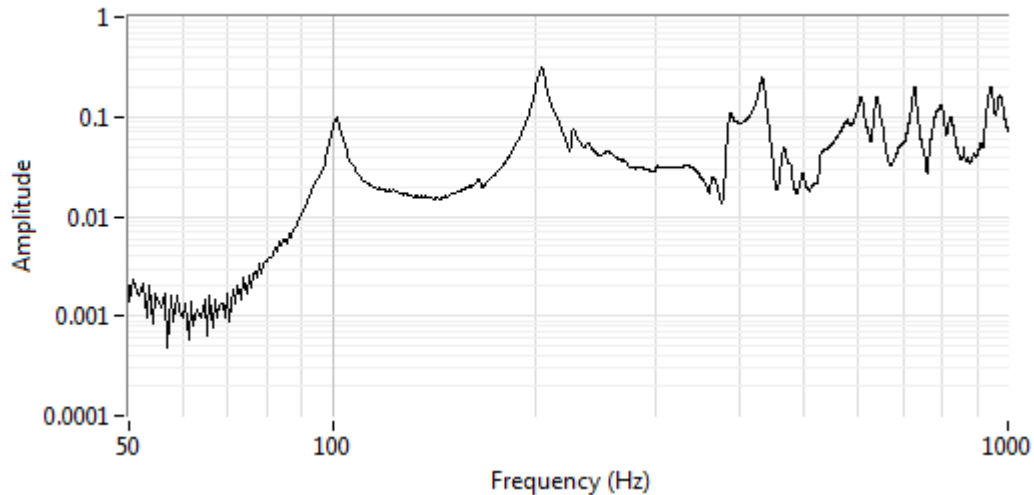


**Figure 4.1.8 FRF from a fully constructed guitar (Yamaha FG-710)**

Figure 4.1.8 demonstrated the FRF from the guitar test, in this measurement the microphone was placed at 5cm away from the guitar and was pointed to the soundhole. The strings on the guitar were muted, where the presence of strings was to apply tension on the guitar. We obtain two distinct peaks at 100 Hz and 200 Hz, which represent the fundamental mode of the airflow and body. This result also has a good agreement with previous studies (Soundhole mode: 90-110 Hz and Plate mode: 180-210 Hz) [2][3]. One of the biggest changes over the FRF is the magnitude at lower modes were significantly amplified. FRF from measuring the guitar top the has a much smaller response in lower modes than the higher modes (Figure 4.1.3). One interesting observation from this result is that the second mode tends to be the octave of the first mode so that this mode might be the combination of the plate and the octave of the soundhole mode.

Since the first two peaks were the result of two coupled acoustic sources, we'd like to investigate how each of these sources behave and how they interacted with each other. Our first question was what if we place the microphone at different locations, both along horizontal and vertical directions.

As we described in Chapter 3, the guitar itself is more likely a double source system, which the soundhole and top plate both can radiate sound. Therefore, the acoustic characteristics from these two sources may have significant differences. In this test, the microphone was placed at different locations (both vertically and horizontally), to measure the sound pressure. The variation in the vertical direction was to see the difference between the sound hole and plate response. The variation in the horizontal direction was to indicate when the doublet model became monopole model, where the difference along the vertical direction disappeared.

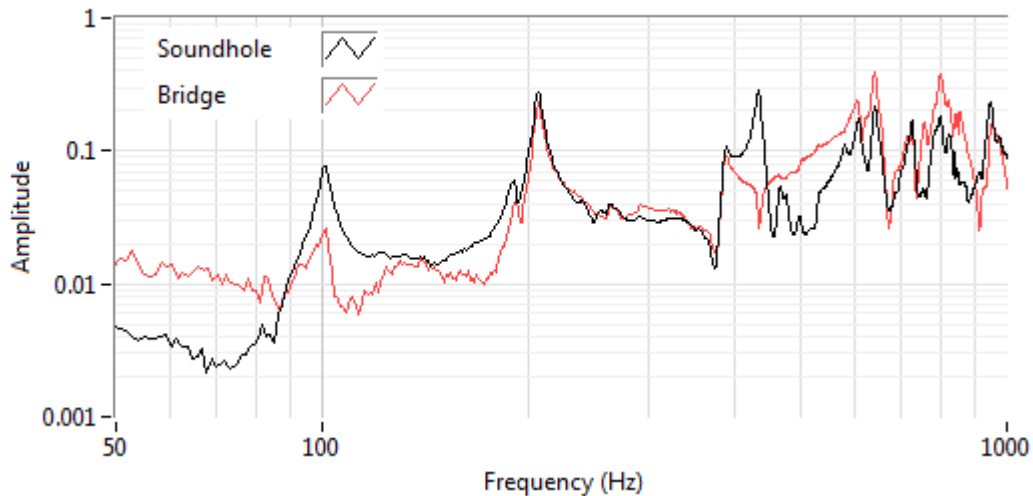


**Figure 4.1.9 FRF measured at 5cm**

The first measurement we did was to compare the difference between measuring the response with pointing the microphone to the soundhole and the bridge. The horizontal distance between the microphone and the guitar is 5 cm, which is much less than the distance between the center of the soundhole and the center of the lower bout plate.

Figure 4.1.9 shows the result of this measurement. As we expected, the first mode was much higher when pointing the microphone to the soundhole. The plate responses from these two measurements were nearly identical. This graph also helped us to identify which source contributed to the overtones, which in this case the response at 430 Hz might be the overtone of the soundhole and responses at 640 Hz and 800 Hz might be primarily from the plate.

Figure 4.1.10 demonstrates the same case but putting the microphone 30 cm away from the guitar. The first mode from two measurements became almost identical, and the first body mode was slightly higher when pointing the microphone to the bridge. The response at 430 Hz still show a significant difference, but overall the variation from these two measurements was much smaller comparing with the previous case, which indicated the guitar started to behave as a single source oscillator.

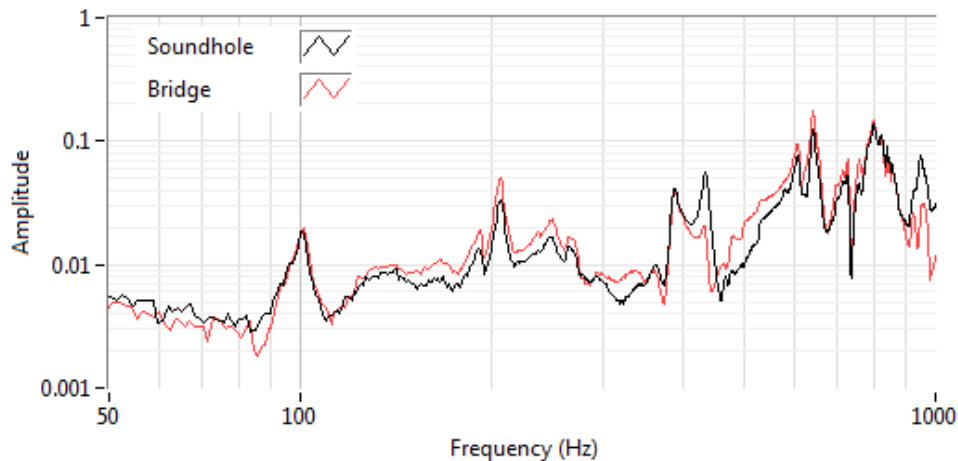


**Figure 4.1.10 FRF measured at 30 cm**

As we move the microphone farther away from the guitar, variation from pointing the microphone to different sound sources could be ignored. Figure 4.1.11 shows the result when we put the microphone 50cm away from the guitar. Even though there are still

some variations (500-600 Hz) along the response function, but we can see the fact that FRF starts to overlap each other.

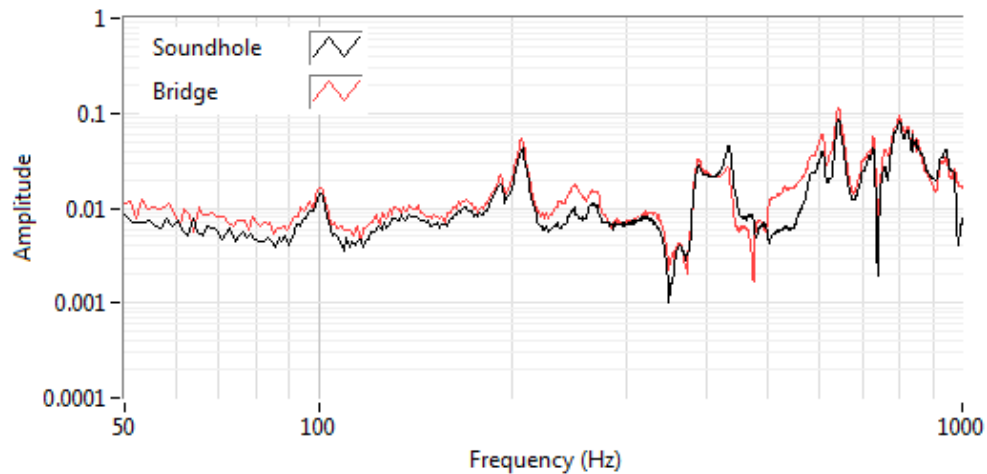


**Figure 4.1.11 FRF measured at 50 cm**

Another approach to investigating the behavior of the top plate mode was done by covering the soundhole with cardboard. A square piece of cardboard was cut and used to cover the soundhole area. The frequency response in this configuration was obtained and showed in Figure 4.1.12. This result was obtained with the microphone pointed to the bridge and left 5 cm away from the guitar, and it was compared with data obtained when the soundhole was not blocked. The biggest change on the FRF was that by covering the soundhole, the response at first mode (breathe mode) dropped dramatically, which indicated the acoustic energy radiated from the soundhole was removed. Another interesting result occurred at the second mode, which also has a reduction on the magnitude with the peak frequency slightly shifted toward to the lower values.

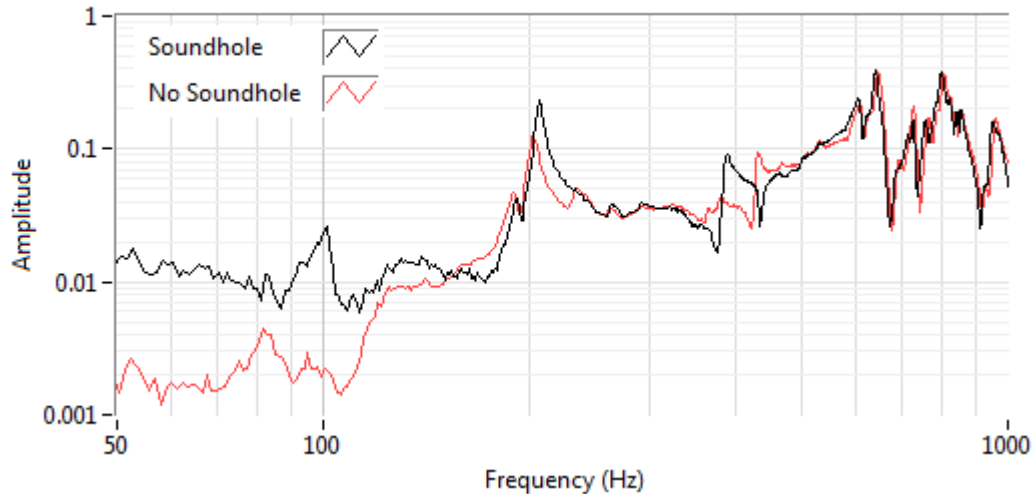


Figure 4.1.12 Effect of covering the soundhole (White: Soundhole is covered, Red: Soundhole is not covered)

In addition to exploring the plate response, we also tried to obtain the FRF when the soundhole plays the dominant role. This task was done by placing the microphone inside the soundhole. The result of this measurement is shown in Figure 4.1.13. When the microphone was inside the guitar, the responses of the first two modes were much higher than the case when the microphone was 5 cm away from the soundhole. Higher modes around 400 Hz showed a significant boost as well, which indicated a strong interaction between the air flow in the body and the plate vibration.

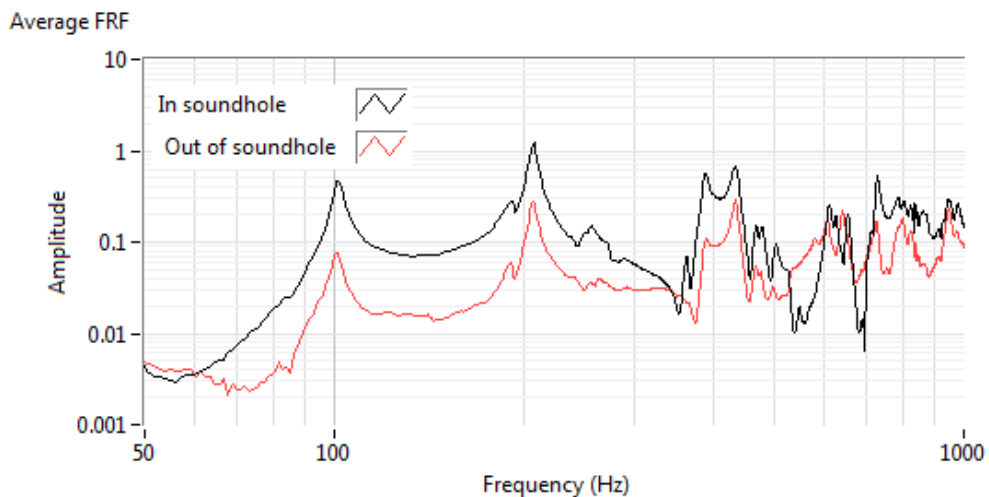


Figure 4.1.13 Effect of placing microphone inside the guitar

As we mention in Chapter 2, we can not ignore the motion of the back plate due to its significant contribution to the air flows. We conducted measurements by putting clays on the back. The presence of clay tends to suppress the motion of the back thus we can evaluate the difference between the free moving back and the suppressed back. The clay bars were deployed in two configurations (Figure 4.1.14) to see their differences. In the first pattern, we One put these clay bars in the center area of the back. In another configuration, we spread the clay bars over the area of the back plate. Figure 4.1.15 shows the result of this measurement. The total mass applied on the back was the same.



Figure 4.1.14 Back plate treatment (left: pattern 1, right pattern 2)

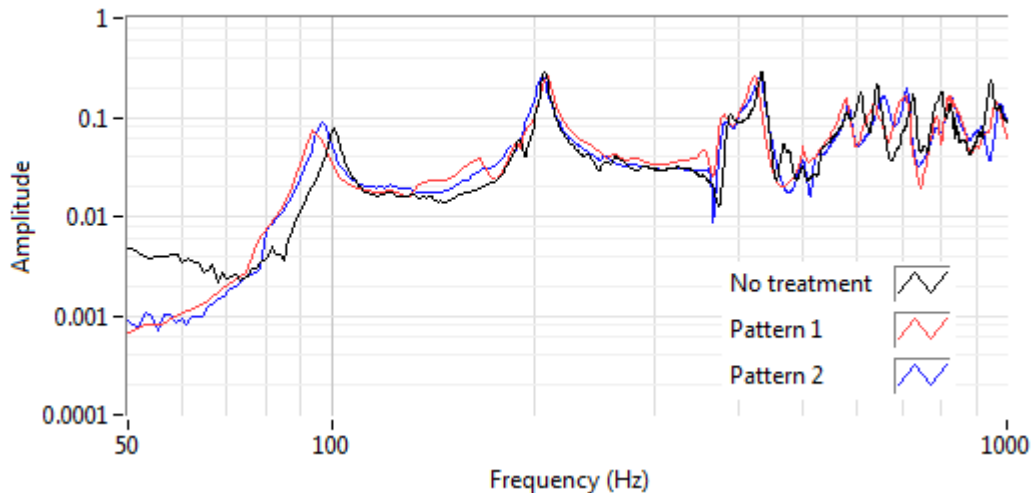
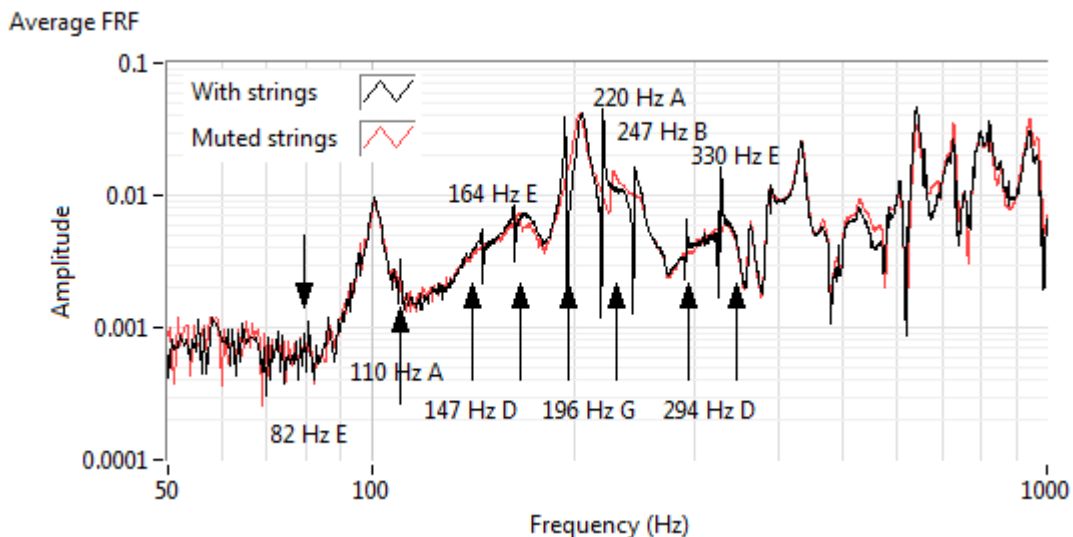


Figure 4.1.15 FRF when the back is damped by clay bars

The biggest effect of the treated back was that the soundhole mode was shifted significantly compared with the plate mode. The resonance frequency has the largest

variation in Pattern 1, where the mass was concentrated at the center. As the mass spread out, the difference became less significant. The body mode did not experience this resonance shift since its primary source is the top plate. We could also observe the shift of the resonance at the soundhole harmonics, such as mode around 430 Hz.

After we tested the how locations could affect the collected frequency response function, we then measured the effect of the strings, where in previous case we muted the string by placing tissues underneath the strings. Figure 4.1.16 shows the comparison between the cases where the guitar was excited with and without muting the strings. Sharp peaks on the white curve could be easily identified at corresponding open string frequencies ( $E_6$ : 82 Hz, A:110 Hz, D: 147 Hz, G:196 Hz, B:247 Hz and  $E_1$ : 330 Hz). The rest of the sharp peaks are primarily the octave of these fundamental notes (165 Hz, 220 Hz, and 294 Hz). The sharp shape of these string notes represents a longer decay period comparing with the vibration of the body, which has much higher decay rate.



**Figure 4.1.16 FRF with without muting the strings (Red: string was muted, Black: strings was not muted)**

Above 330 Hz, the string response disappeared, which is most likely due to the higher damping rate at those harmonic frequencies. As we mentioned earlier, the string tension



could potentially affect the frequency response of the guitar. In Figure 4.1.17, we demonstrate the effect after we removed the strings. The presence of string tension does not have an obvious effect on the soundhole mode in the FRF. However, it slightly changed the frequency of the plate mode (~3Hz). Results from previous tests showed variations mainly on the magnitude, and no obvious frequency shift was observed. Therefore, we believe this slight shift was from the tension of the string.

This section demonstrated all our testing results, in next section, we will have some more detailed interpretations regarding these outcomes.

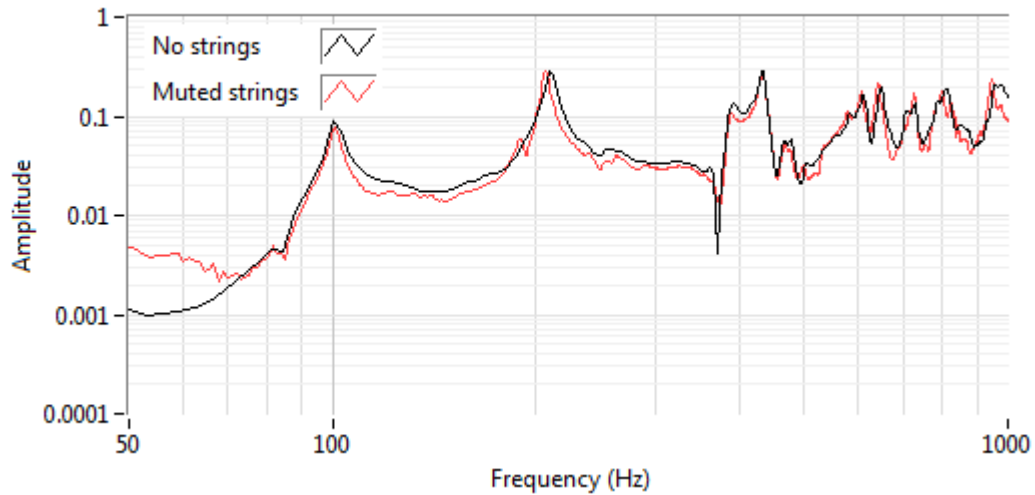


Figure 4.1.17 Effect of the string tension

## Chapter 4.2 Discussion

The most useful indication from testing the guitar top was that the bracing reduced the magnitude variation at higher frequencies, which is usually a good sign for a musical instrument to deliver a uniformed response. For analyzing the lower modes, we adapted Caldersmith's [3] proposition that we can assume the vibration area of the top has a circular shape located at the lower area of the the guitar top (Figure 4.2.1). The radius corresponding to this proposition was measured, and this distance was used to calculate the resonance mode using the method introduced by Rossing [20].

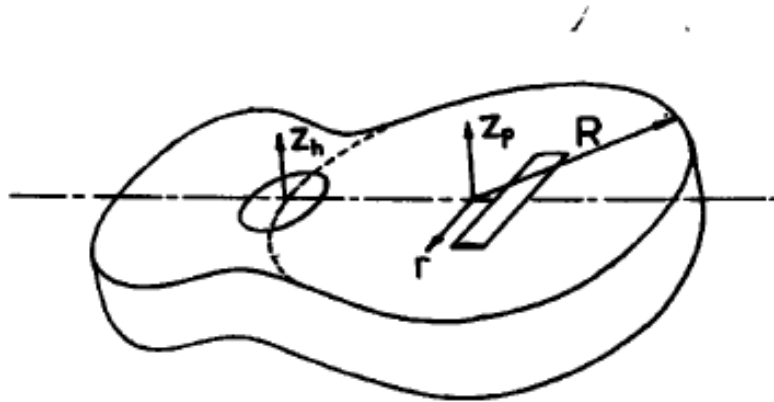


Figure 4.2.1 Assumed vibrational area of the guitar top (source: Caldersmith [3])

In this calculation, we adopted the fixed boundary condition, and the first resonance frequency of a clamped circular plate could be calculated as

$$f_1 = 10.216\sqrt{D}/R^2$$

Where  $h$  is the thickness of the top, and  $A$  is the area measured as shown in Figure 4.2.1.  $D$  is the flexural rigidity of the board, which is calculated as

$$D = \frac{Eh^3}{12(1-\nu)}$$

$E$  is the Young's modulus of the  $\nu$  top and is the Poisson's ratio. The fundamental mode for a circular plate with hinged boundary (simply supported) condition is calculated as

$$f_1 = 4.977\sqrt{D}/R^2$$

where the two constant 10.216 and 4.977 are the eigenvalues from the solution of the Bessel's function.

Table 4.2.1 lists the result from this calculation. These calculated values were compared with the center frequency of the first resonance plateau from the unbraced situation.

Table 4.2.1 Estimation of the fundamental mode using circular & fixed boundary assumption

Spruce		
E	1.10E+10	pa
Poisson's ratio	0.3	
Thickness	0.0025	m
R	0.18	m
D	1580	Pa*m <sup>3</sup>
f01 clamped	210	Hz
f01 (simply supported)	97	Hz
f01 measured	173	Hz

We have a significant variation between the calculated values and the measured value, which means we cannot simply model the case with either assumption. Some factors could contribute to this difference. The first one is from the mechanical properties of the wood, where grain tends to have higher stiffness along its growing direction and is less stiff across its growing direction. The second factor could be the geometry itself, where the shape of the guitar board is much complicated than a simple circle. Another influential factor could be boundary conditions.

The FRF of the guitar did not show distinct peaks except modes at around 170 Hz 400 Hz. This response curve is mostly because the nature of the plane vibration. Another reason is that the decay of the measured signal was fast which made the spectral analysis harder.

Therefore, we tried also to measure a fully constructed guitar to see how the enclosed body transformed the FRF of the top.

The guitar used in this study has the same top wood as our naked board to minimize the variation from using different materials. Figure 4.2.2 shows the comparison between the FRF of the naked board and the guitar. In this figure, we can see how the added body could change the response of the guitar system.

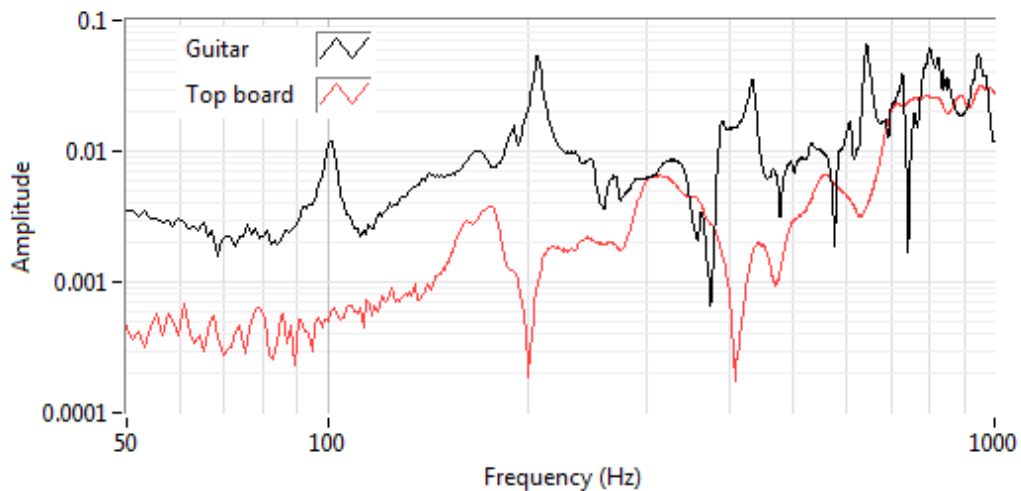


**Figure 4.2.2 FRF of the top and guitar**

The most obvious effect of the guitar body is that it greatly amplified the lower frequency response. The fundamental resonance of the plate was also shifted toward to the higher frequency. Another difference is that the shape of these responses also changed, where the guitar tended to have sharper peaks. As we mentioned in Chapter 3, the shape of the response is usually a good indication of the decay of the signal. Figure 4.2.3 shows the time domain signal of the guitar board and the guitar with same microphone location, where the signal from the naked board decay much faster than the guitar. We can also observe that the signal has a smooth decay envelope so that we know we don't have significant reverberations.

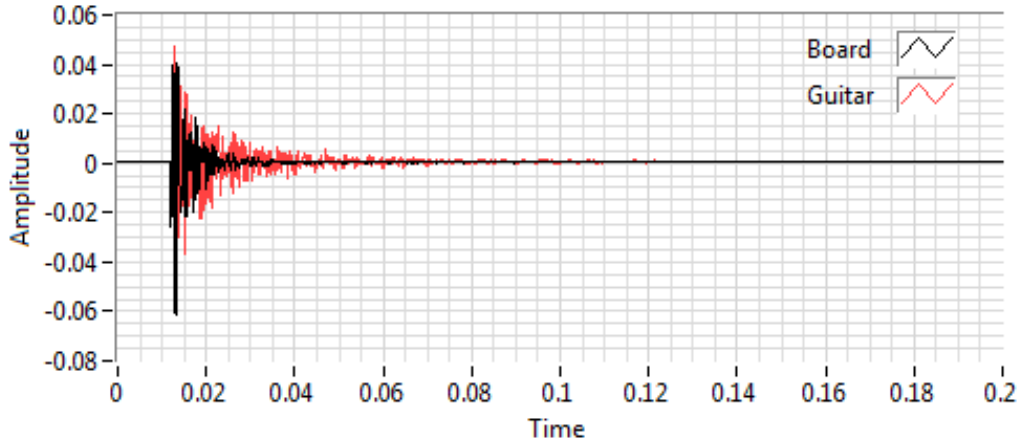


Figure 4.2.3 Time-domain signal of the board and guitar signal

After we obtained the FRF of the guitar, next we tried to evaluate the damping property of the measured signal. The basic methodology was described in Chapter 3.1, where Q factor is evaluated as

$$Q = \frac{f_c}{\Delta f}$$

And the damping coefficient is

$$r = \frac{\omega_0}{2Q}$$

Table 4.2.2 and 4.2.3 list the key values from evaluating the first two modes of the guitar FRFs. The distance in the table indicates the horizontal location of the microphone where each case was evaluated by pointing the microphone to the source.

Table 4.2.2 Q factor of the sound hole mode at various distance (Microphone pointing to the soundhole)

Soundhole mode	5cm	30cm	50cm
Power	0.095	0.02	0.015
Frequency (Hz)	101	101	101
Upper limit (Hz)	103	104	104
Lower limit (Hz)	98	97	94
Q	20.2	14.4	10.1
Damping	2.5	3.5	5

Table 4.2.3 Q factor of the Plate mode at various distance (Microphone pointing to the bridge)

Plate-mode	5cm	30cm	50cm
power	0.34	0.055	0.055
frequency (Hz)	206	206	206
upper (Hz)	211	212	212
lower (Hz)	203	202	202
Q	25.8	20.6	20.6
Damping	4	5	5

The Q factors of the soundhole mode show a decreasing trend as the microphone move away from the source, which means the acoustic energy tends to decay faster with the increase of distance. The Q factors of the plate mode were smaller than soundhole cases in short distances, but they reached the same value when the microphone was at 50 cm from the guitar. Also, the Q factor of the plate mode did not change significantly with the increase of distance, along with the non-uniform change of the magnitude so that the near-field effect may be still dominant.

It is also interesting to investigate how the sound hole could affect the Q factor of the plate mode, which could show the evidence of the coupling effect. Table 4.2.4 lists these data for the two cases. By covering the soundhole, both the power magnitude and the plate resonance frequency were changed. This effect was mostly because of the coupling effect between the two, and they also agreed with the result from Christensen [2], who stated the actual plate mode will have a lower resonance frequency. A higher quality factor in the uncovered soundhole case shows that the air oscillation through the soundhole is supporting the plate vibrating, which makes it last longer.

Table 4.2.4 Comparison of the presence of the soundhole (Microphone was 5cm away from the source)

Plate-mode	Soundhole uncovered	Soundhole covered
power	0.34	0.12
frequency (Hz)	206	203
upper (Hz)	211	207
lower (Hz)	203	197
Q	25.8	20.3
r	4	5

We also evaluated the Q factor where the microphone was placed inside the soundhole, and the result is shown in Table 4.2.5. The biggest change from putting the microphone inside the soundhole was that led to a dramatic boost to the magnitude of the response (even greater than 1). This phenomenon again proves that the enclosed body is the main resonator where the pressure has the highest fluctuation. The Q factor did not vary significantly compared with when the microphone was outside the body, which implied the system impulse response is consistent, and our initial assumption to the system is valid.

Table 4.2.5 Q factor when the microphone was placed in the soundhole

In soundhole	Soundhole mode	Plate mode
power	0.43	1.2
frequency (Hz)	101	207
upper (Hz)	104	212
lower (Hz)	98	202
Q	16.8	20.7
r	3	5

The result from testing the effect of the soundhole, back plate, and string tension provided valuable information for us to understand how these components could affect the final frequency response of the instrument. The soundhole effect might be adjusted by

varying the depth of the body and the size of the soundhole. Treatment could also be done to the backplate, where non-uniform thickness plate could be applied. The purpose of these adjustments was to obtain the two clear responses at lower modes and a more balanced response to higher modes.

We were using the averaged FRF all of our analysis. However, the actual measurement uncertainty involved in our measurement might not be revealed after we took the averages. Therefore, our uncertainty analysis was conducted by calculating the square root of the deviation to the averages at each frequency, which is

$$\sigma_r = \frac{\sqrt{\frac{1}{N} \sum_{i=1}^N (x - \bar{x})^2}}{\bar{x}}$$

This value will indicate the ratio between the absolute measurement uncertainty and the average magnitude where the sample size (N) here is 15. Figure 4.2.4 shows the uncertainty of the measurement in Figure 4.1.4, where the response of the guitar top was measured with different pickup locations. At low frequencies (<300 Hz), the error shows a positive relationship with the distance of the microphone. Uncertainties in this region show a great impact from the background noise (fluctuations). At higher frequencies, particularly between 300 Hz to 400 Hz error was dramatically reduced and all cases have similar relative errors. However the relative uncertainty becomes large again above 500 Hz and values from three cases were no longer consistent. The highest occurred at 600 Hz in the 120 cm case, where has a steep drop of power in the spectra.

The relative variation in measuring the guitar responses were also calculated, which is plotted in Figure 4.2.5. Compare with the uncertainty from measuring the top, it was significantly smaller, and it also shows the uncertainty tends to increase with the increase



of the microphone distance. All three cases showed a higher relative error around 400 Hz, where is the harmonic of the soundhole mode. Also, the relative uncertainties measured at higher frequencies were more consistent in measuring the guitar, which implied the guitar is much easier to characterize than the naked board.

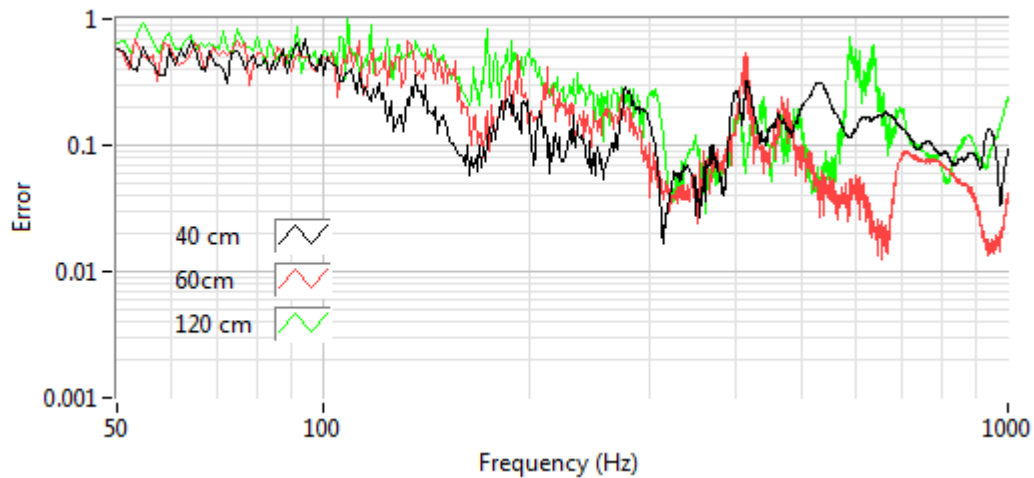


Figure 4.2.4 Error in guitar board measurement

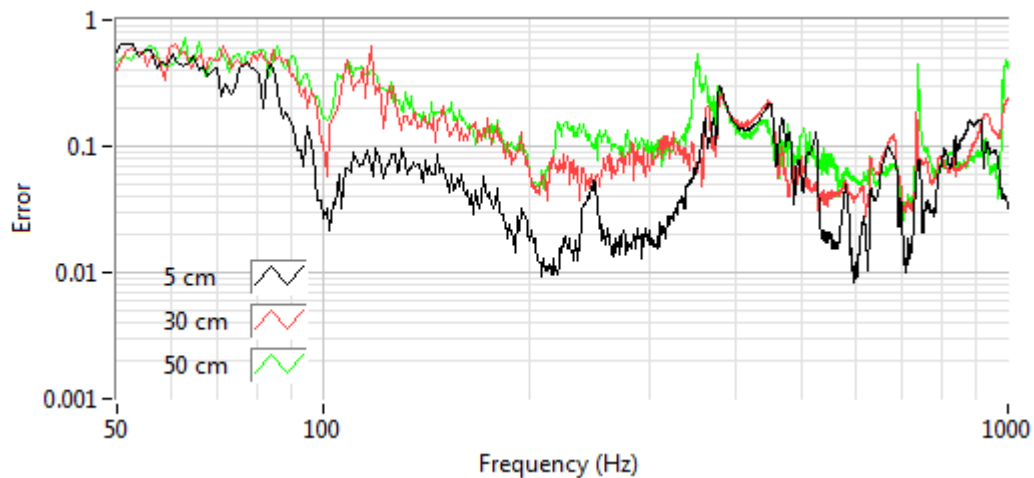


Figure 4.2.5 Error in guitar measurement

The result from the error analysis indicates even though we conducted the test in a relatively quiet area, low-frequency noise is still the primary source to affect our measurement. So in future studies, we might need to do some improvement to the environment if we want to measure the free field signal. Also in testing the guitar board,

our method might not be the best choice since the boundary condition was not consistent. The original thought was trying to keep the measurement as simple as possible. However our result convinced us that some work has to be done in future tests to improve data collection. For example, in testing the top board, it is better to clamp it with some frames that can exert a uniform boundary condition. Also continuous power injection (power speaker or shaker) could also be introduced to investigate the power spectrum of the top board response in addition to solely measuring the frequency response.

## Conclusion

In this study, we measured the frequency response function of an X-braced guitar top and a fully constructed guitar with the same top bracing pattern. The original purpose of this study was trying to see if we could use a simple method to characterize the guitar top to assist guitar maker in the tuning process. The result from testing the guitar top indicated the effect of the X-bracing, which it might suppress some of the lower responses but significantly smooth the higher responses. However, our result did not agree well with the theoretical value, which one reason might be because theoretical models are simple (simple geometry and homogeneous material) and another reason might be our testing method was not sufficient to characterize the guitar top, especially the related boundary condition was not consistent along the edge.

The result from measuring the guitar shows a good agreement with past studies. Compare with the top board response, the effect of the enclosed body mainly boosts the response of these lower modes. Two distinct peaks were observed, which the first peak around 100 Hz is the soundhole mode and the second peak around 200 Hz are the plate mode. At time-domain, the added body will reduce the decay rate of the plate mode, which is a good indication of the coupling effect. These could also be represented by the Q factor of these two peaks in the frequency domain. The soundhole mode was significantly suppressed when we cover it with a cardboard. Also, both the magnitude and frequency of the plate changed, which showed a reduction of the coupling effect. While putting additional weight on the back, the frequency of the soundhole mode shifted to lower values. The plate mode would be slightly affected by the applied tension from the strings.

Response from measuring the different radiating source (soundhole and plate) might be useful in acoustic-electric guitars designs since we observed significant variation in the frequency response when we pick up sound from different sources. Therefore, it might be worth to try to install pickup at both locations, which is similar to the electric guitar so that players can adjust the tone based on their preferences.

Uncertainty analysis showed that the low-frequency noise was still the primary source that contributed to our measurement error, where this is especially true when we move the microphone away from the source. Therefore, in the future test, a larger and quieter space might be required if we want to measure the free field response.

### **Future Works**

This research only revealed a small portion of the nature of the acoustic guitar. In the future, we expect to explore more influential parameters such as the dimension of the top plate (area, thickness), the area of the soundhole, the shape of the bracing stick, bracing patterns, the size of the enclosed body, properties of the bridge and material of sides and back. However, this is hard to test each combination of the configuration, even in using numerical simulations. Therefore, a dimensionless (or similarity) analysis would be a more promising solution. The benefit of similarity solution is that it will lump many parameters to a dimensionless number (such as Reynolds number commonly seen in fluid mechanics) to describe the system response. In this case, guitar makers could quickly check the parameters, they need to achieve given guitar tones.

Another issue was raised by the high expense of the tools. Therefore, an open source platform with lower cost hardware would be a better approach to guitar makers and musicians. For example, the sensors could be connected to a microcontroller or a

microcomputer, and then we can create a program that can read the data and conduct same analysis using open source tools. Or a server program could be run on the computer that can send the result to the internet immediately after the measurement.

## Reference

1. R. Boullosa, "Vibration measurements in the classical guitar," *Applied Acoustics*, Volume 63, Issue 3, pp. 311-322, March 2002
2. G. W. Caldersmith and E. V. Jansson, "Frequency Response and Played Tones of Guitars," *STL-QPSR*, Volume 21, pp. 50-61, 1980
3. G. Caldersmith, "Guitar as a Reflex Enclosure," *Journal of Acoustic Society of America*, Vol 63, No 5, pp. 1566-1576, May 1978
4. O. Christensen, "Quantitative Models for Low Frequency Guitar Function," *Journal of Guitar Acoustics*, Volume 6, No 2, pp. 10-25, Sept 1982
5. I. Cutur and M. Stanciu, "Modal Analysis of Different types of Classical Guitar," *Proceedings of the 10th WSEAS International Conference on Acoustics & usic: Theory & Applications, A TA'09. World Scientific and Engineering Academy and Society (WSEAS), Stevens Point, Wisconsin, USA*, pp. 30-35.
6. D.P. Hess, "Frequency Response Evaluation of Acoustic Guitar Modifications," *Savart Journal*, Vol 1, No 3, July 2013
7. P. Dumond, and N. Baddour, "Effects of using scalloped shape braces on the natural frequencies of a brace-soundboard system," *Applied Acoustics*, Volume 73, Issue 11, pp. 1168-1173, November 2012
8. F. Fahy "Foundation of Engineering Acoustics," Beccles, Suffolk, UK, Paston PrePress Ltd, ch 3, sec 6-10, pp. 26-39, 2001
9. I. Firth, "Guitars: Steady State and Transient Response," *Journal of Guitar Acoustics*, Issue 6, No 4, pp. 42-49, Sept 1982
10. I. Firth, "Physics of the Guitar at the Helmholtz and First Top Plate Resonances," *Journal of Acoustic Society of America*, Volume 61, No 2, pp. 588-593, Feb 1977
11. M. French, "Response Variation in a Group of Acoustic Guitar", *Sound and Vibration* 42, No 1, pp. 18-22, January 2008
12. M. French, "Technology of the Guitar," New York, Springer, 2012, pp. 79-84, 235
13. T. Huber and N. Beaver, "Non-Contact Modal Excitation of a Classical Guitar Using Ultrasonic Radiation Force," *Journal Experimental Techniques*, Vol 37, Issue 4, pp. 38-46, June 2011
14. L. Kinsler and A. Frey, "Fundamental of Acoustics", 4<sup>th</sup> edition, New York, John Wiley& Sons, pp. 284-285
15. J. Lai, and M. Burgess, "Radiation Efficiency of Acoustic Guitars," *Journal of Acoustic Society of America*, Volume 88, Issue 3, pp. 1222-1227, Sept 1990
16. Leissa, "Vibration of Plate," NASA SP-160, pp 1-10, Chapter 1
17. N.E Molin and E.V Jansson, "Transient wave propagation in wood plate for musical instruments," *Journal of Acoustic Society of America*, Vol 85, No. 5, pp. 2179-2184, May 1989
18. A. Oppenheim, "Signals and Systems," 2<sup>nd</sup> edition, Pearson Education, pp. 423-482, 2009
19. Olson, Harry, "Music, Physics and Engineering," New York, Dover Publications, pp. 65-75,114-116, 1997
20. T. Rossing, "Plate Vibration and Application to Guitars," *Journal of Guitar Acoustics*, Issue 6, No 7, pp.65-73, Sept 1982
21. S. Sali and F. Hindryckx, "Modeling and Optimizing of the First Guitar Mode," *Savart Journal*, Vol 1, No 1, pp1-13, June 2011

22. *W. Strong, "Studying a Guitar's Radiation Properties with Nearfield Holography," Journal of Guitar Acoustics, Issue 6, No 5, pp. 50-59, Sept 1982*
23. *A. Torres, and R. Boullosa, "Influence of the Bridge on the Vibration of Top of a Classical Guitar," Applied Acoustics, Volume 70, Issue 11-12, pp.1371-1377, Dec 2009*